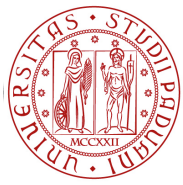

UNIVERSITÀ
DEGLI STUDI
DI PADOVA

Sede Amministrativa: Università degli Studi di Padova

Dipartimento di Biologia

SCUOLA DI DOTTORATO DI RICERCA IN : Bioscienze e Biotecnologie
INDIRIZZO: Genetica e Biologia molecolare dello sviluppo
CICLO XXV

The role of the clock gene *Bmal1* in skeletal muscle

Direttore della Scuola : Ch.mo Prof. Giuseppe Zanotti
Coordinatore d'indirizzo: Ch.mo Prof. Paolo Bonaldo
Supervisore :Ch.mo Prof. Gerolamo Lanfranchi

Dottorando : Marcia Ivonne Peña Paz

31 Gennaio 2013

"Choose a job you love, and you will never have to work a day in your life"

Confucius

TABLE OF CONTENTS

Acknowledgements ..... **iii**

Abbreviations ..... **v**

1 SUMMARY **1**

1.1 English **1**

1.2 Italian **2**

2 AIM OF THE PROJECT **4**

3 Introduction **5**

Circadian rhythms in mammals **5**

3.1 Molecular aspects of the clock machinery **6**

3.2 Posttranslational modifications that regulate the circadian machinery **9**

3.3 The central pacemaker and peripheral clocks. **11**

3.4 External regulation of circadian rhythms **12**

3.5 The muscle clock **13**

4 Materials & Methods **14**

4.1 Mice **14**

4.1.1 *MLC1f*−Cre 14

4.1.2 *HSA*−Cre 14

4.1.3 $Bmal1^{fl/fl}$ 15

4.2 Genotyping **16**

4.3 Sample collection **18**

4.4 RNA **18**

4.4.1 Microarray 20

4.4.2 RT−qPCR 20

4.5 Protein methods: Western blotting **21**

4.6 Histology **23**

4.6.1 Cryosections 23

4.6.2 Histochemistry 23

4.6.3 Immunofluorescence 24

4.6.4 Electron microscope preparation 25

4.7 *In vivo* muscle force measurements **26**

4.8 Statistical analysis **27**

5 Results **28**

5.1 *Bmal1*$^{fl/fl}$ x *MLC1f*−Cre mice 28
5.1.1 Characterization of the animal model 28
5.1.3 *Bmal1* mKO phenotype 30
5.1.4 Locomotor activity 34
5.1.6 Force measurements 35
5.2 Gene expression profile 36
5.2.1 Altered pathways 41
5.3 *Bmal1*$^{fl/fl}$ x *HSA*−Cre (Inducible knockout) 44
5.3.1 Preliminary characterization 44
5.3.2 Lifespan, body weight and muscle weight 45
5.3.3 Circadian rhythms of locomotor activity 46
5.3.4 Force measurements 47

6 Discussion 49
6.1 *Bmal1* deletion in whole body and in skeletal muscle 49
6.2 The effect of *Bmal1* mKO on the muscle core clock 49
6.3 BMAL1 and MyoD 50
6.4 *Bmal1*, muscle structure and muscle function 50
6.6 p38 pathway 52
6.7 Future perspectives 53

References 55

ACKNOWLEDGEMENTS

This thesis would not have been possible without the guidance and the help of different people that have contributed in many different ways during the preparation of this work.

First I would like to express my gratitude to Prof. Stefano Schiaffino for the opportunity of letting me work under his supervision, and for his help and advice during the three years of PhD. I would also like to thank the lab for all the help they have given me. In particular I would like to thank Ken Dyar for the opportunity to work within his project, Bert Blaauw because he was always encouraging me to be a better scientist, Stefano Ciciliot for always being there when I did not know what to do, Alberto Rossi for introducing me to the lab and its techniques and helping me be independent, Lisa Agatea because she made our work in the lab easier, Francesca Solagna because even if it was difficult to work together we managed to get along well, and Judith Ceelen because she was an exemplary student who became a good friend and a great listener. I also take this opportunity to thank Mattia and Lisa from Avogaro's group, and Giulia, Vanina and the rest of Sandri's group because they have always been helpful.

I cannot express in words my gratitude to Mamá for her hard work and example, without her I would not be able to do this job, and to Papá that even from the distance has always been there. Thanks also to Andrés y Alejandro - even though we argue we have each other's back. To Abuelita for her words of wisdom, and the rest of the family because they have always been there for me in the time I needed.

I am lucky to have friends that make my life happier and are a big support, because of that I want to thank my dear Lauren for being there during the times that I wanted to quit, for telling me to keep going and offering to kick the world for me, for her scientific advice, for our meetings at the bar to talk about my writing, and because we would spend long hours talking about science or 'il gatto'. I thank Vikki for providing me with food and wine while I was writing, and her valuable scientific advice and nice chats. I thank my MUZIC fellows for

the scientific discussions, advice and all the plans for the future. I am grateful to Ari who became my sister during this time, and to Dragana for pushing me to enjoy life. I want to thank Cris because even if we were in different countries our conversations encouraged me to be brave and take advantage of the opportunity I was given. I would also say thanks to Paty, Laurent, Mariella, Belén and Sergio for worrying about me when I was not reachable. Lastly, I am thankful to D&D for the random chats and for making me laugh.

I would also like to acknowledge the FP7−European MUZIC consortium for providing me with funding, and for the excellent training opportunities.

I wish it were possible to thank all the people that have crossed my path and have left a print on me, helping me become the person I am. I can just say thanks for being part of my life.

¡GRACIAS!

ABBREVIATIONS

bHLH: basic-helix-loop-helix

Bmal1 imko: *Bmal1* muscle specific inducible knockout

Bmal1 mko: *Bmal1* muscle specific knockout

BMAL1: brain and muscle aryl hydrocarbon receptor nuclear translocator (arnt) like

BSA: bovine serum albumin

CLOCK: circadian locomotor output cycles kaput

DEPC: diethylpyrocarbonate

DTT: DL- dithiothreitol

EDL: extensor digitorium longus

EDTA: ethylenediaminetetraacetic acid

GA: gastrocnemius

GSEA: gene set enrichment analysis

HCl: hydrochloric acid

HRP: horseradish peroxidase

HSA: human skeletal actin

$MgCl_2$: magnesium chloride

MLC1f: myosin light chain 1f

NaCl: sodium chloride

NaF: sodium fluoride

$NaVO_3$: sodium orthovanadate

PCR: polymerase chain reaction

PVDF: polyvinylidene fluoride

RHT: retino-hypothalamic tract

RT−qPCR: real time- reverse transcription quantitative PCR

SCN: suprachiasmatic nucleus

SDS: sodium dodecyl sulphate

SOL: soleus

TA: tibialis anterior

TAM: tamoxifen

ZT: zeitgeber time

1 SUMMARY

1.1 English

Circadian rhythms are responsible for various rhythmic 24-hour changes in physiological and behavioral parameters. A core oscillator located in the suprachiasmatic nucleus (SCN) of the hypothalamus is responsible for the coordination of these rhythms. The SCN controls the endogenous timing system by coordinating the tissue-specific clocks present in all cells of the body. The regulation is mainly based on a core transcriptional-translational feedback loop that keeps internal gene expression entrained by the external light-dark cycle. The transcription factor *Bmal1* is a major component of both central and peripheral clocks, and its absence leads to disruption of circadian rhythms.

In order to understand the function of the intrinsic muscle clock we compared two muscle specific knockouts of the *Bmal1* gene (a conditional model *Bmal1* mKO and an inducible model *Bmal1* imKO) and their normal wild type littermates. Changes in muscle phenotype were analyzed at morphological and physiological level, and muscle gene expression was determined.

We have observed that in contrast with the whole body *Bmal1* knockout, *Bmal1* mKO mice have a normal lifespan and growth. Contrary to the extreme muscle atrophy found in *Bmal1* null mice, muscle-specific *Bmal1* mKO causes a small but significant increase in muscle mass. However, this hypertrophic phenotype is not accompanied by an increase in muscle force, and indeed there is a marked reduction in both absolute muscle force and muscle force normalized to muscle weight. Myofibrillar architecture is conserved in *Bmal1* mKO muscles, and there are no major histological abnormalities in the muscles. Myosin heavy chain composition is slightly shifted to fast myosin heavy chain isoforms. We have compared the muscle circadian gene expression profile of these mice and their control littermates. Our analyses indicate that the transcription of many circadian muscle genes is greatly altered. By Gene Set Enrichment Analysis (GSEA) we found that the p38 pathway, including upstream activators

and downstream targets, is down−regulated, suggesting that this pathway, which is known to be linked to contractile activity, is controlled by BMAL1.

1.2 Italian

I ritmi circadiani sono responsabili della variazione giornaliera di molteplici parametri fisiologici e di comportamento. L'orologio centrale preposto alla coordinazione di questi ritmi è localizzato nel nucleo soprachiasmatico dell'ipotalamo. Il nucleo soprachiasmatico scandisce il ritmo globale dell'organismo sincronizzando il ritmo dei cosiddetti orologi periferici dei tessuti, presenti in tutte le cellule del corpo. La regolazione avviene principalmente tramite un circuito accoppiato di trascrizione-traduzione, che mantiene l'espressione genica interna vincolata al ciclo esterno di luce e buio. Il fattore di trascrizione *Bmal1* è uno dei principali componenti sia dell'orologio centrale che di quelli periferici, e la sua assenza porta alla scomparsa dei ritmi circadiani nell'organismo.

Al fine di comprendere la funzione dell'orologio intrinseco del muscolo, abbiamo confrontato due diverse linee di topi in cui il gene *Bmal1* è assente esclusivamente nel muscolo scheletrico (un modello condizionale, nominato *Bmal1* mKO, e un modello inducibile, chiamato *Bmal1* imKO), con dei topi di controllo appartenenti allo stesso ceppo selvatico. Cambiamenti fenotipici a livello muscolare sono stati analizzati sia a livello morfologico che fisiologico, ed è stata inoltre valutata l'espressione genica globale del muscolo.

Abbiamo così osservato che a differenza dei topi in cui il gene *Bmal1* è assente in tutte le cellule del corpo (*Bmal1*$^{-/-}$), i topi *Bmal1* mKO hanno una durata della vita ed una crescita normale. Al contrario della forte atrofia riscontrata nel topo *Bmal1*$^{-/-}$, nel nostro modello muscolo-specifico *Bmal1* mKO abbiamo rilevato un significativo, benché piccolo, incremento di massa muscolare. Ad ogni modo, ciò non è accompagnato da un aumento della forza muscolare ne' assoluta, ne' normalizzata rispetto al peso del muscolo. L'architettura del muscolo è preservata nei topi *Bmal1* mKO, e questi non presentano anomalie vistose a livello istologico. Nei topi *Bmal1* mKO si nota un leggero incremento nel numero delle

fibre che esprimono catene pesanti delle miosine di tipo rapido. Abbiamo inoltre confrontato l'espressione genica circadiana di questi topi rispetto ai loro controlli. Le nostre analisi indicano che la trascrizione di molti geni circadiani muscolari è fortemente alterata. Tramite analisi di arricchimento di gruppi genici (*Gene Set Enrichment Analysis*, o GSEA), abbiamo trovato che la via di segnalazione della proteina p38, inclusi attivatori a monte e bersagli a valle, è ridotta, suggerendo così che questa via, nota per essere legata all'attività contrattile, sia controllata da BMAL1.

2 AIM OF THE PROJECT

BMAL1 is a transcription factor of the basic-helix-loop-helix PAS domain family, known to be an essential part of the molecular clock that regulates circadian rhythms. A mouse model lacking BMAL1 in the whole body has been previously generated and has the following phenotype: completely disrupted circadian rhythms, shortened lifespan, decreased body weight and muscle weight, and impaired muscle function (weaker muscles) (Bunger *et al.,* 2000; Kondratov *et al.,* 2006; Boden *et al.,* 2006; McDearmon *et al.,* 2006; Andrews *et al.,* 2010). However, it is not clear whether the changes in skeletal muscle are due to the lack of BMAL1 in muscle cells or are secondary to the disruption of circadian rhythms in other tissues. In order to understand the importance of *Bmal1* in skeletal muscle, we generated and characterized two mouse models with a depletion of *Bmal1* specifically in skeletal muscle using the Cre−LoxP system. The first model was a conditional muscle−specific knockout (*Bmal1* mKO) and the second model was an inducible muscle−specific knockout (*Bmal1* imKO).

In summary, our objective was to elucidate the effect of the local muscle disruption of *Bmal1* without altering the clock machinery in the rest of the body.

3 INTRODUCTION

Circadian rhythms in mammals

The term circadian comes from the Latin '*circa*' and '*diem*', which mean approximately a day. Circadian rhythms are thus regular biological processes with a period of approximately 24−hours. All organisms are subject to daily environmental changes, such as day and night cycles due to the Earth's 24−hour rotation around its axis, that makes them adapt to the different conditions during the day and night.

The presence of an internal clock in organisms helps them to prepare for these changes in the environment, allowing them to adapt to but also to anticipate daily variations in environmental conditions. These biological clocks are synchronized to external time by various timing cues. While the most prominent environmental signal is the light, other relevant cues, such as temperature, feeding and activity rhythms may also entrain the endogenous clock.

In mammals, the core pacemaker in the suprachiasmatic nucleus (SCN) of the hypothalamus receives direct innervation from the retina, and coordinates physiological functions with the light/dark cycle. Peripheral clocks present in all cells of the body are ultimately synchronized by circulating factors and neural cues (**Figure 1**).

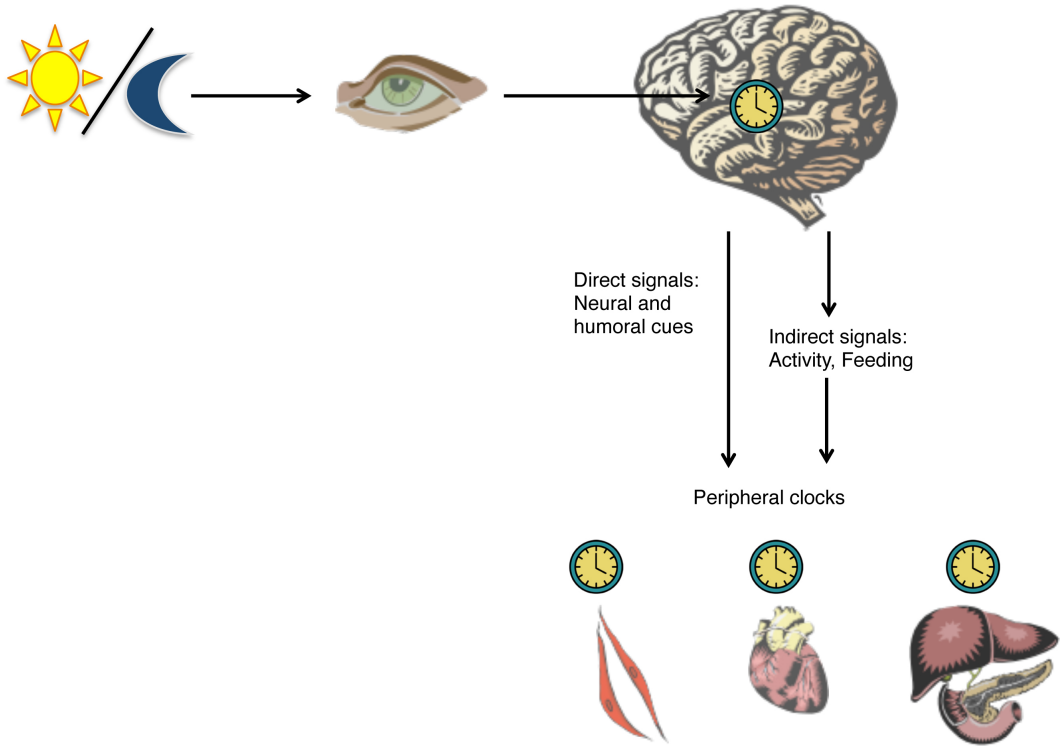

Figure 1. Hierarchical organization of the biological clock in mammals

3.1 Molecular aspects of the clock machinery

Circadian rhythms are finely regulated and the mechanism of regulation is based on a conserved transcriptional−translational feedback loop that is self−autonomous, and is present in all the cells of the body (**Figure 2**).

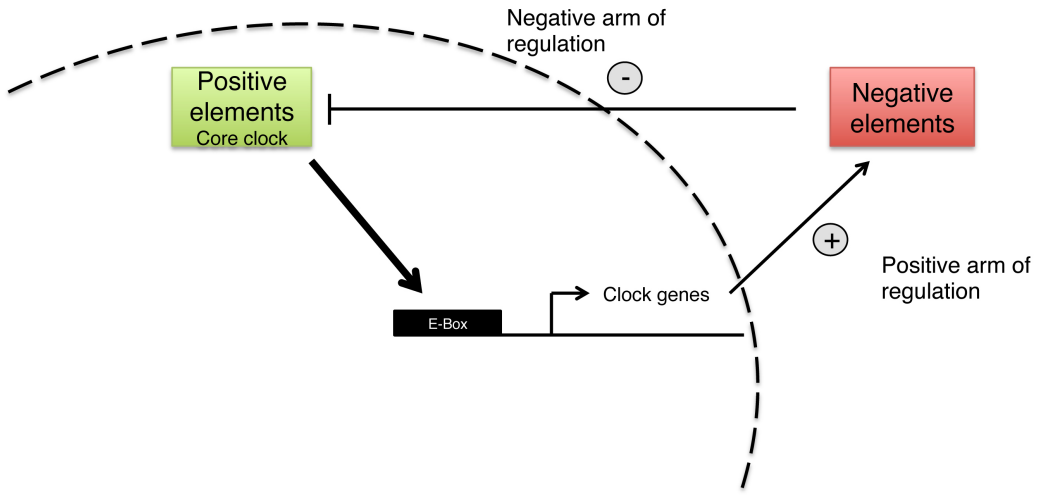

Figure 2. Scheme of the transcriptional−translational feedback loop composed of both the positive and negative arms of regulation that is present in all cells of the body. Adapted from (Albrecht, 2007).

The main components of the clock machinery are circadian locomotor output cycles kaput (CLOCK) protein, Brain and Muscle Aryl hydrocarbon receptor nuclear translocator−like protein1 (BMAL1), Period (PER1, PER2, and PER3), and Cryptochrome (CRY1 and CRY2).

CLOCK and BMAL1 are transcription factors from the basic−helix−loop−helix Per−Arnt−Sim (bHLH−PAS) family. They form heterodimers and comprise the core component of the clock (Hogenesch *et al.,* 1998), which regulates the transcriptional activation of target genes that have E−boxes in their promoters (with the consensus sequence CACGTG) such as the mammalian *Period (Per)* and *Cryptochrome (Cry)* genes (Gekakis *et al.,* 1998). This forms the positive arm of regulation of the feedback loop that activates the target genes *Per*, *Cry*, *RORα*, *REV−ERBα*, and other clock−controlled genes. The negative arm of regulation of the feedback loop is formed by PER and CRY proteins, that accumulate gradually and form heterodimers that migrate into the nucleus repressing the formation of CLOCK:BMAL1 complex. PER2 positively regulates *Bmal1* transcription, whereas CRY1 or CRY2 inhibit the transcriptional activity of BMAL1 when it is in complex with CLOCK (Shearman *et al*., 2000; Griffin *et al.*, 1999). It is a finely−tuned feedback loop in which the mRNA levels of both arms of the loop accumulate in an anti−phase manner allowing the cycle to oscillate in a 24−hour period.

The primary feedback loop is regulated by a secondary stabilizing feedback loop that coordinates circadian expression of *Bmal1*, and is composed of two of orphan nuclear receptors REV−ERBα and β, and RORα, β and γ. The *Bmal1* promoter has recognition sequences (ROREs) for REV−ERB and ROR. The RORE consensus sequence is (A/T)A(A/T)NT(A/G)GGTCA, and has been shown to give a cyclic gene expression profile (Ueda et al 2002). REV−ERBα is a repressor of *Bmal1* expression, which is activated by the CLOCK:BMAL1 complex, and which presents an oscillatory mRNA expression profile with an opposite phase to that of *Bmal1*. It was shown that mice lacking REV−ERBα have elevated levels of BMAL1 causing a disrupted rhythm of activity with shorter cycle (Preitner *et al.,* 2002). In contrast, RORα has a role in the transcriptional activation and maintenance of *Bmal1* levels but not in its rhythmic expression.

It was also shown by Sato *et al.,* that mice lacking RORα have reduced levels of BMAL1, indicating a positive influence of RORα on *Bmal1* expression (Sato *et al.,* 2004). The authors report that there is a competition between REV−ERBα and ROR for the binding to the *Bmal1* promoter's ROR element in order to regulate *Bmal1* expression, and it is directly linked to the amount of each protein. However, it seems that REV−ERB repressor may exert a more prevalent role compared to the ROR activators. When the REV−ERB protein levels decrease, ROR enhances the transcriptional activation of *Bmal1* and maintains its robust oscillation (Akashi & Takumi, 2005).

The stabilizing loop also acts on different levels: it has been reported that the CLOCK:BMAL1 complex not only regulates *Cry1* directly, but also indirectly via REV−ERBα (which, as said previously, is a repressor of *Bmal1* expression). It has been suggested that E−box and ROR elements in the *Bmal1* gene contribute to the precise tuning of the circadian timing system, and the second feedback loop plays a role in the control of the clock output genes (Liu *et al.,* 2008).

In addition to the secondary loop formed by REV−ERB and ROR, other interlocking loops include the PARbZIP family of transcription factors, including DBP, HLF, and TEF, and putative PARbZIP antagonist E4BP4. These are directly regulated by the core clock through E−boxes on their promoters, and act on target genes. E4BP4 (also called NFIL3) was reported to be a negative regulator of clock output genes, whereas the PARbZIP family members are activators of the transcriptional activity of output genes, and they show an anti−phase pattern of expression. The PARbZIP proteins and E4BP4 share a similar conserved binding sequence RT(G/T)AYGTAAY, where R is a purine and Y a pyrimidine, and they regulate target genes in a complementary manner. A model was proposed, in which the CLOCK:BMAL1/PER:CRY complexes directly regulate PARbZIP family members, which in turn regulate clock−controlled genes. For E4BP4, there is an indirect regulation of the core clock machinery, through REV−ERBs and RORs. It was also shown that the activity of PAR proteins and E4BP4 may feed back to the core clock machinery, as was reported *in vitro* in the regulation of *Per1* (Mitsui *et al.*, 2001; Asher & Schibler, 2011). DBP was reported to increase the transcriptional activation of *Per1* upon the activation by the core clock, as part

of the interlocking loops. *Dbp* has also been reported to be negatively regulated by CRY (Yamaguchi *et al.,* 2000)

The final advantage of having interlocking loops would be to maintain the persistence and period of the cycle in spite of external perturbations, while transducing the external cues into the molecular clock and being able to efficiently adapt (**Figure 3**) (Liu *et al.,* 2008).

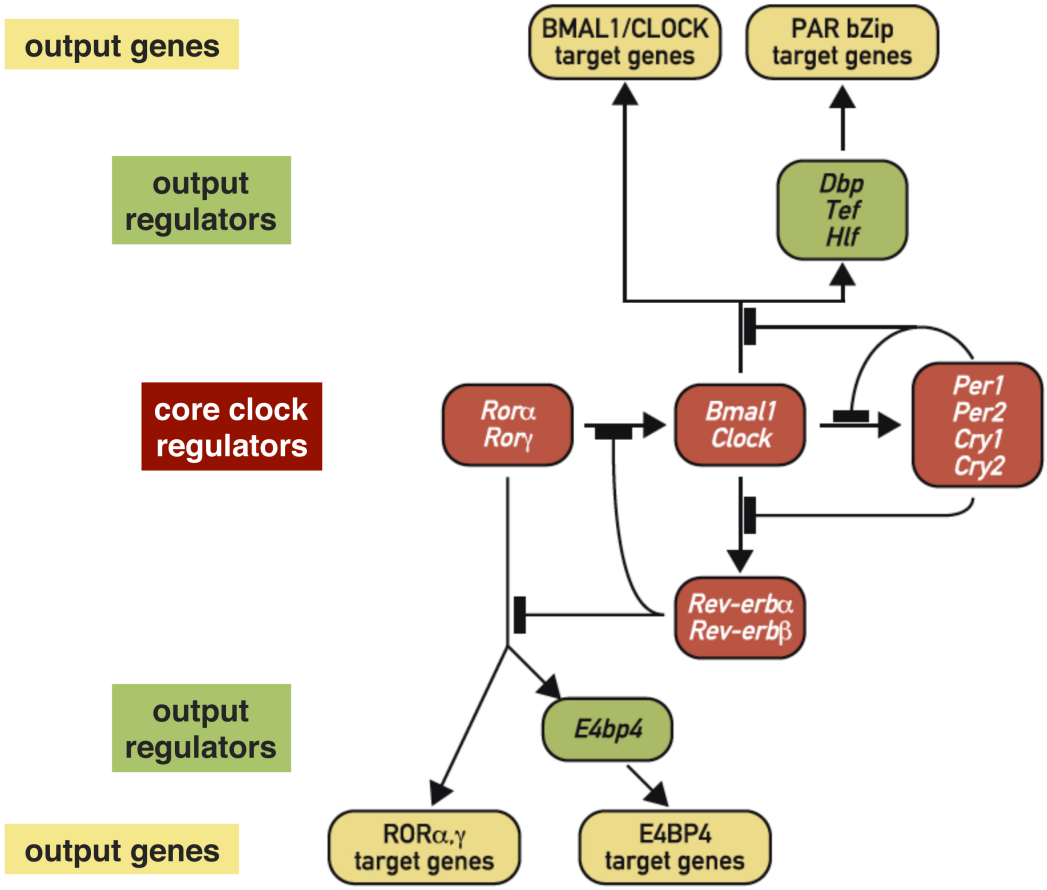

Figure 3. Schematic representation of the molecular clock. The primary feedback loop is formed by positive elements CLOCK and BMAL1 and the negative elements PER and CRY. The secondary feedback loops are formed by clock−controlled genes that act as regulators of the core clock or second regulators of clock−controlled genes. Figure adapted from (Asher & Schibler, 2011)

3.2 Posttranslational modifications that regulate the circadian machinery

In order to keep the 24−hour cycle, it is important to maintain the delay between the positive and negative arms of the clock. This is achieved by introducing

posttranslational modifications that regulate nuclear import and export, chromatin accessibility and also protein degradation (Gallego & Virshup, 2007).

The core clock protein BMAL1 is phosphorylated by Casein Kinase I delta and epsilon (CKIδ and CKIε), and this promotes CLOCK:BMAL1 dependent transcription (Eide *et al.,* 2002). It has been reported that mutations in CKI have an effect on circadian rhythmicity. For example, the *tau* hamster has a mutation in CKIε and shows a shortened locomotor activity period (Lowrey *et al.*, 2000). Also, in humans mutations of CKI have been associated with a disruption of period length, causing familial advance sleep−phase syndrome (FASPS) (Jones *et al.,* 1999). Period proteins are also phosphorylated by CKI promoting their degradation by the ubiquitin−proteasome pathway (Vanselow *et al.,* 2006). CRYs are also a substrate for CKIε when bound to PER1/2, yet the functional significance is unknown (Eide *et al.*, 2002; Takano *et al.*, 2000).

Additionally, the mitogen activated protein kinase (MAPK) phosphorylates BMAL1 in different sites, thus impairing the binding of the CLOCK:BMAL1 complex to the promoter of target genes (Sanada *et al.,* 2002). It was also shown that the p38 MAPK pathway indirectly activates the promoter of *Per1* by phosphorylation of the cAMP responsive element binding protein (CREB), however this activation does not play a role in the regulation by CLOCK:BMAL1 (Travnickova−Bendova *et al.,* 2002).

BMAL1 rhythmicity is also controlled by the addition of small ubiquitin−related modifier proteins, after the activation of CLOCK:BMAL1 targets, thus regulating the turnover of the protein (Cardone *et al.,* 2005).

Finally, the F−box protein FBXL3 a component of the Skp1 Cullin F−box (SCF) E3 ubiquitin ligase complex has been identified as a component of the circadian machinery, stabilizing the equilibrium between activation and repression of CLOCK:BMAL1 complex through the turnover of CRY. Ubiquitination of CRY by FBLX3 leads to a decrease in inhibition of the CLOCK:BMAL1 complex, controlling the circadian homeostasis (Godinho *et al.*, 2007; Siepka *et al.*, 2007; Busino *et al.*, 2007).

3.3 The central pacemaker and peripheral clocks.

The retina perceives light and then sends the signal via the retino−hypothalamic tract (RHT) to the SCN that acts as the coordination center of the 24−hour rhythm. The SCN is a self−sustained oscillator, which mantains a robust rhythmicity even in the absence of light. Through neural and humoral pathways the SCN communicates with the rest of the body, entraining all cells to the light/dark cycle, controlling gene expression rhythms and various physiological and metabolic parameters. Synchronization between the SCN and the peripheral tissues is fundamental for phase coherence within the timing system. The SCN normally sends timing signals to the periphery, entraining self−sustained clocks in peripheral tissues to external time (Balsalobre *et al.*, 2000). When the SCN is lesioned, there is a persistent circadian oscillation of the peripheral clocks that is sustained in time but it is no longer in phase between different cells or tissues. This demonstrates that, while the peripheral clocks are able to function independently, the SCN is needed to ultimately synchronize the phase of all clocks (Yoo *et al.,* 2004).

Early experiments in rats showed that lesions in the suprachiasmatic area and not the preoptic area of the brain lead to disruption of activity and drinking behavior (Stephan & Zucker, 1972). It was later demonstrated by rescue experiments in hamsters that implanting fetal SCN grafts into SCN−lesioned animals restored normal locomotor activity rhythms (Lehman *et al.,* 1987). These studies focused attention on the SCN as the crucial point that transmits light information to the rest of the body. Mammals perceive the light via the retina of the eye. Distinct ganglion cells that express the photopigment melanopsin gather the photic information that is transduced through axonal projections along the RHT (Berson *et al.,* 2002). In response to this signal, the RHT terminals release glutamate and pituitary adenylate cyclase−activating peptide (PACAP) at synapses with SCN neurons. This photic input activates signaling pathways, causing chromatin remodeling and inducing a rapid expression of clock genes (Albrecht *et al.*, 1997; Sun *et al.*, 1997). *Per1* activation has been shown to be the first to occur: an activation of the extracellular−signal regulated kinase (ERK) phosphorylates CREB, which acts as a transcriptional activator of *Per1* by

binding to the CRE motifs in its promoter (Travnickova−Bendova *et al.,* 2002). The SCN projects to and thus transmits information to other nuclei within the brain via different neurotransmitters. The entrainment of other brain nuclei allows for further transmission of circadian information via neural and hormonal cues that that control various behavioral and physiological functions, including feeding behavior, body temperature and locomotor activity, ultimately entraining peripheral tissues to the 24−hour cycle (Dibner *et al.,* 2010).

3.4 External regulation of circadian rhythms

Feeding time has been demonstrated to a major entrainment factor for circadian rhythms in peripheral tissues. For example, when nocturnal mice (which normally eat during the night) are subjected to restricted feeding during the day, they display a phase resetting of peripheral clocks. Animals under restricted feeding show a decrease in body temperature during the night that may be the cue for the changes in the peripheral tissues but not in the SCN that is not affected by these variations. The liver is the first organ to adapt to the shift in food intake, responding to metabolites and hormonal levels (Damiola *et al*., 2000; Stokkan *et al.*, 2001).

In vitro experiments in rat−1 fibroblasts have reported that treatment with glucose synchronizes circadian gene oscillation. It was observed that the metabolism of glucose regulates *Per1*, *Per2*, and *Bmal1* through glucose responsive immediate early genes *Tieg1* and *Vdup1*. TIEG1 negatively regulates *Per1* and *Bmal1* genes acting on Sp1 sequences present in their promoters. VDUP1 is a negative regulator of thioredoxin, a DNA binding partner of various transcription factors that enhances the activity of HIF1α and HLF promoting their interaction with CREB−Binding protein, which mediates CLOCK:BMAL1 complex activation, therefore VDUP1 may negatively regulate CLOCK:BMAL1 complex and reduce *Per1* and *Per2* transcription (Hirota *et al.,* 2002).

3.5 The muscle clock

Locomotor activity is often used as a readout of circadian rhythms, but it is unknown whether circadian rhythms entrain locomotor activity, or if the activity affects the entrainment of the peripheral clock machinery. Similar to other peripheral tissues, skeletal muscle contains local clocks and responds to circadian neural cues like motor neuron activity, as well as responding to the central SCN clock.

It has been reported that disrupting the circadian machinery via knockout of the clock gene *Bmal1* in mice may lead to an altered phenotype that includes reduced lifespan, lower bodyweight, reduced activity and reduced force production. This decrease in body mass is accompanied by a striking reduction in muscle mass and muscle fiber size (Kondratov *et al.,* 2006). Surprisingly, rescue experiments in the *Bmal1*$^{-/-}$ mice showed that specific expression of *Bmal1* in skeletal muscle restores muscle mass and activity levels, whereas rescuing *Bmal1* expression in the brain only restored rhythmic patterns of activity (McDearmon *et al.,* 2006). Furthermore, it was reported that the clock machinery regulates muscle integrity, as *Bmal1*$^{-/-}$ mice were reported to have disorganization of the sarcomeric structure, and decreased force production (Andrews *et al.,* 2010).

4 MATERIALS & METHODS

4.1 Mice

All experimental protocols were reviewed and approved by the local Animal Care Committee, Università degli Studi di Padova. All mice used were from a C57BL/6 background. Pups were weaned four weeks after birth and house according to sex. Mice were housed approximately six to a cage, with food and water *ad libitum* in a 21ºC controlled facility under a 12h light/dark cycle (12:12 LD).

4.1.1 *MLC1f*−Cre

These mice express the Cre recombinase under the control of the myosin light chain 1 f promoter (*MLC1f*), in fast and slow skeletal muscle starting from early postnatal stages (Bothe *et al.,* 2000).

4.1.2 *HSA*−Cre

These mice express Cre recombinase linked to a mutated estrogen receptor (CreER) driven by the Human Skeletal Actin (*HSA*) promoter, which is selectively active in fast and slow skeletal muscles (Schuler *et al.,* 2005). In this line, Cre recombinase activity is normally inactive, but can be induced at a desired time by treatment with the synthetic estrogen receptor ligand 4−hydroxytamoxifen (tamoxifen or TAM). In the absence of TAM, the CreER is localized in the cytoplasm. When TAM is administered, it binds to the mutated ER, causing the CreER translocation to the nucleus and induce activation of Cre recombinase, thus allowing for the recombination and deletion of any regions of genes flanked by LoxP sites.

4.1.3 *Bmal1*$^{fl/fl}$

These mice were purchased from Jackson laboratories (B6.129S4−*Arntl*^{tm1Weit}/J). They contain LoxP sites flanking the exon coding for the basic−helix−loop−helix domain (bHLH) of *Bmal1*. Mice homozygous for this *Bmal1* mutant allele are indistinguishable from wild type mice (Storch *et al.,* 2007). Animals carrying the mutant allele have wild type activity of BMAL1, but when the allele is excised animals carry a null mutation of *Bmal1*.

Mice breeding

For the conditional *Bmal1* muscle specific knockout (*Bmal1* mKO), *Bmal1*$^{fl/fl}$ mice were crossed with *MLC1f*−Cre mice, obtaining a first generation of mice heterozygous for both the floxed *Bmal1* allele and the *MLC1f*−Cre allele (BM1). BM1 mice were crossed a second time with *Bmal1*$^{fl/fl}$ mice in order to obtain homozygous mice for the *Bmal1*$^{fl/fl}$ allele and heterozygous for the Cre allele (BM2). For successive generations these mice were backcrossed to the original *Bmal1*$^{fl/fl}$ line. The resulting *Bmal1* mKO mice were always compared to their Cre negative control littermates (**Figure 4**A).

For the inducible *Bmal1* muscle specific knockout (*Bmal1* imKO) the same method was used, breeding the *Bmal1*$^{fl/fl}$ line with the *HSA*−Cre line. After obtaining the *Bmal1*$^{fl/fl}$ expressing the CreER, adult mice were treated for 5 days with tamoxifen (one daily intraperitoneal injection of 1 mg tamoxifen in 10% (v/v) ethanol/sunflower oil) to induce the deletion of the exon encoding for the bHLH domain of the *Bmal1* gene. *Bmal1* imKO mice and their Cre negative control littermates were analyzed one month after TAM treatment (**Figure 4**B).

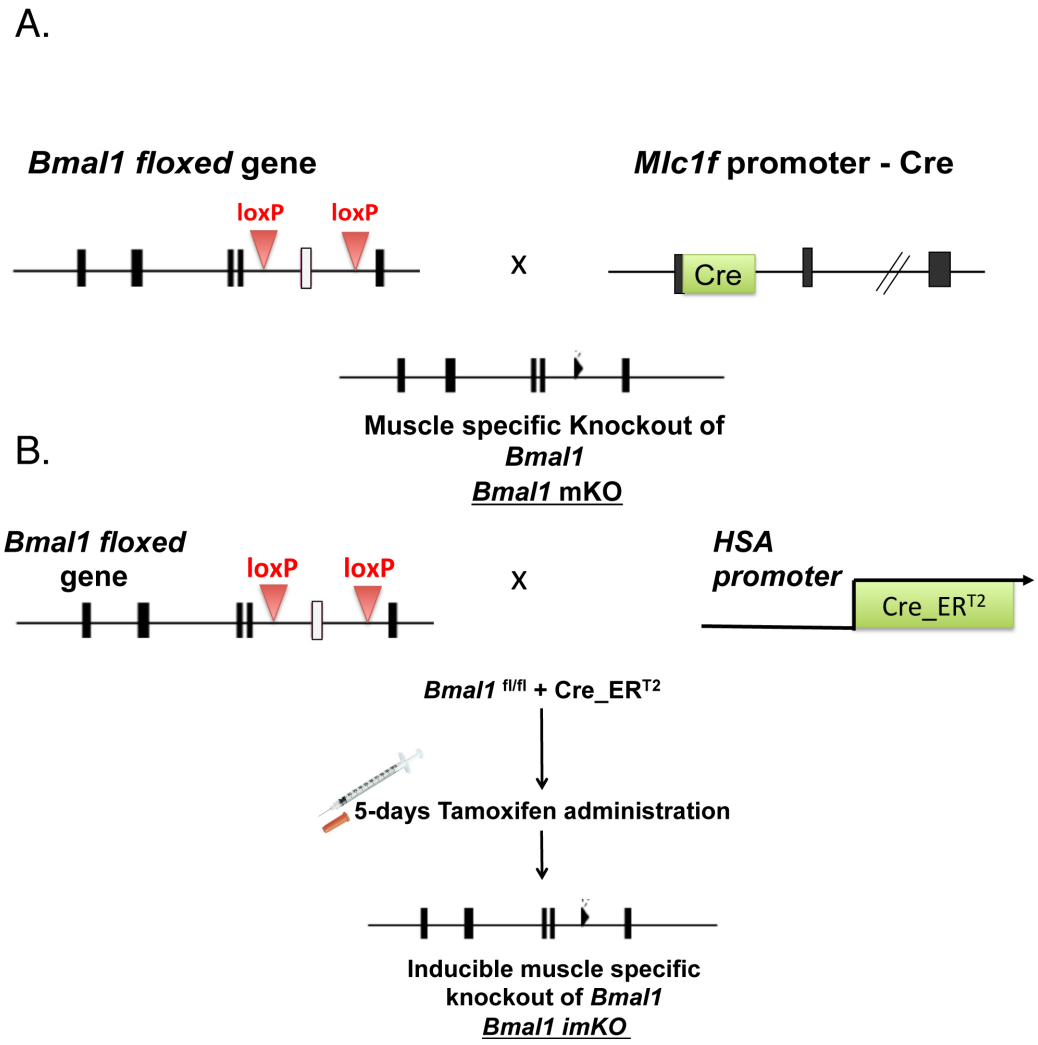

Figure 4. Schematic representation of the knockout models. A. Conditional *Bmal1* muscle specific knockout, crossing of the transgenic line with the *Bmal1* floxed gene (exon 9 is flanked by two LoxP sites) and the line that expresses the Cre recombinase under the MLC1f promoter. The litters that we obtained from this cross are skeletal muscle specific KO for *Bmal1*. B. Conditional *Bmal1* inducible muscle specific knockout; the *Bmal1* floxed line is crossed with the HSA promoter driven Cre recombinase, the knockout is then induced in adult animals by the administration of tamoxifen

4.2 Genotyping

Mice pups, approximately one to two weeks of age were numbered according to our mouse identification scheme providing an ID for each mouse. A small tissue sample was biopsied for genomic DNA isolation.

Genomic DNA isolation buffer

100mM Tris HCl pH 7.5
200µg/ml Proteinase K
DNA isolation protocol

Extraction of DNA

Biopsies were placed in 50µl of genomic DNA isolation buffer; samples were heated to 57ºC for one hour for the DNA extraction, after which the samples were brought to 99ºC to inactivate the proteinase K. The genomic DNA was stored at −20ºC until used.

Genotyping PCR

For the characterization of the inherited *Bmal1* and Cre alleles a standard polymerase chain reaction protocol was followed. A mix containing Taq polymerase and buffers was used (GoTaq Green Master mix 2x, Promega). Forward and reverse primers (**Table 1**) were added to a final concentration of 0.1µM, with 1µl of the isolated genomic DNA solution.

Gene	Primer	Sequence 5' → 3'	Primer Type
Bmal1	oIMR7525	ACT GGA AGT AAC TTT ATC AAA CTG	Forward
	oIMR7526	CTG ACC AAC TTG CTA ACA ATT A	Reverse
Cre	NSP−780	CAC CAG CCA GCT ATC AAC TCG	Forward
	NSP−979	TTA CAT TGG TCC AGC CAC CAG	Reverse

Table 1. Sequences of the primers used for the genotyping of the mice

Thermal profile for *Bmal1* PCR:

1) 94°C for 3min
2) 94ºC for 30sec
3) 56ºC for 1min
4) 72ºC for 1min
5) 35 cycles of steps 2 to 4
6) 72ºC for 1min
7) 10ºC hold

The size of the amplified fragments is expected to be 327bp for the wild type allele and 431bp for the mutant allele.

Thermal profile for *Cre* PCR

1) 94°C for 3min
2) 94ºC for 45sec
3) 61ºC for 30sec
4) 72ºC for 1min
5) 40 cycles of steps 2 to 4
6) 72ºC for 1min
7) 10ºC hold

The expected amplified fragment size is 200bp.

DNA gel electrophoresis

10µl of the amplified PCR product was analyzed on a 1% (w/v) agarose gel (w/v) stained with EuroSafe (Euroclone) a fluorescent nucleic acid stain. Then the electrophoretic gel is run in TBE buffer at 100V for 1h and visualized by UV light. The ladder used to confirm the expected size of the fragments was either a 100bp ladder or a 2−log ladder (BioLabs).

4.3 Sample collection

Following the ethic committee protocol, animals were sacrificed by cervical dislocation in order to minimize suffering of the mice. Six animals, three controls and three knockouts, were sacrificed at Zeitgeber times ZT0 (lights ON), ZT4, ZT8, ZT12 (lights off), ZT16 and ZT20. Tissues were collected and immediately frozen in liquid nitrogen for RNA and protein assays.

4.4 RNA

RNA extraction

RNA was extracted from frozen muscle samples using TRIZol® (Invitrogen) according to manufacturer's instructions. Briefly, a sample of powdered tissue was taken and homogenized in TRIzol to disrupt all cell membranes and release

RNA, DNA, and protein. Chloroform was used to separate the RNA phase from DNA and protein; total RNA was precipitated with isopropanol and finally resuspended in 30-50µl of DEPC-treated water. Following NanoVue spectrophotometer (General Electrics) determination of RNA concentration, RNA quality was controlled by the absorbance ratio OD260/OD280, with a ratio ≥1.8 RNA was considered acceptable.

RNA retrotranscription

cDNA was obtained from the reverse transcription of the total RNA following the protocol:

5−25ng Random primers
1nM dNTPs
0.8µg RNA
Volume up to 26µl dH_2O

Thermal profile

1) 65ºC for 5min
2) 4ºC hold

Then add:
8µl First strand buffer
2µl of 0.1mM DTT
2µl RNase Inhibitor
2µl SuperScript® III RT (Invitrogen)

Thermal profile

1) 25ºC for 10min
2) 42ºC for 50min
3) 70ºC for 15min
4) 4ºC hold

4.4.1 Microarray

For gene expression profiling, 250ng of RNA from tibialis anterior or soleus muscles was hybridized to Mouse Gene 1.0 ST Arrays (Affymetrix) Three biological replicates were used per group for each time point.

Gene expression data was normalized and summarized with Robust Multichip Average (RMA) using custom Chip Description File (CDF) files (Version 14.1.0; EntrezG) to remap the probes on the arrays to recent genome and transcriptome library data (Dai *et al.,* 2005). Differentially expressed genes were determined using a default R2 threshold of 0.6 and a cubic regression model in maSigPro (microarray Significant Profiles), a two−step regression−based method to identify genes with significant temporal expression changes and significant differences between experimental groups in time series microarray experiments (Conesa *et al.,* 2006). Rhythmic genes that cycle with a 24h period were identified using a Benjamini−Hochberg *Q*−value< 0.2 in the non−parametric algorithm JTK_Cycle (Hughes *et al.,* 2010). Enrichment was assessed using Gene set enrichment analysis (GSEA) (Subramanian, Tamayo *et al.,* 2005) using gene sets from the TRANSFAC and Biocarta databases. Using default settings, gene sets were called significant with a $p<0.05$ and False Discovery Rate (FDR) <0.25.

4.4.2 RT−qPCR

Primer sets were designed using Primer−BLAST (NCBI) and validated by gradient PCR and electrophoretic analysis to test for optimal annealing temperature, reaction efficiency and specificity prior to use.

cDNA samples were amplified on the 7900HT Fast Real−Time PCR System (Applied Biosystems) using the Fast SYBR Green RT−PCR kit (Applied Biosystems). All samples were analyzed in duplicates.

The thermal profile used for the RT−qPCR was:

1) 95ºC for 20sec
2) 95ºC for 1sec
3) 60ºC for 20sec
4) 40 cycles of steps 2 and 3
5) 95ºC for 15sec
6) 60ºC for 15sec
7) 95ºC for 15sec

Specificity of gene amplification was confirmed by analyzing the dissociation curves of the genes (**Table 2**) with SDS 2.4 software (Applied Biosystems). Analysis was performed using the standard curve method and all data were normalized relative to *36B4* mRNA expression.

Gene	Sequence 5' → 3'	Primer Type
mBmal1	GCA GTG CCA CTG ACT ACC AA	Forward
	TCC TGG ACA TTG CAT TGC AT	Reverse
m36B4	TAT GGG ATT CGG TCT CTT CG	Forward
	AGC GGT TTT GCT TTT TCATC	Reverse

Table 2. Sequences of the primers used for the RT−qPCR to confirm the microarray data

4.5 Protein methods: Western blotting

Protein isolation buffer

50mM Tris pH 7.5
150mM NaCl
10mM $MgCl_2$
0.5mM DTT
1mM EDTA
10% (v/v) glycerol
2% (w/v) SDS
1% (v/v) Triton
1mM $NaVO_3$
5mM NaF
3mM Glycerol−2−Phosphate
Complete® 50x (Roche)

Protein isolation:

Proteins were isolated from cryosections of muscle. Muscles were cut in the cryostat and 30 cryosections of 20µm thickness were collected in 1.5ml

vials. 100µl of protein extraction buffer was added trying to cover all cryosections and subsequently placed in ice. Next, samples were vortexed and heated up to 70ºC for 10min with continuous shaking, at approximately 700rpm. After that the vials were centrifuged at 4ºC 13000rpm for 15min. The supernatant was collected and the pellet was discarded. From the supernatant or protein lysate, 2µl was taken for quantification and the remaining protein lysate was stored at −80ºC until use.

Protein quantification:

The protein lysate was quantified using the Bicinchoninic acid kit (BCA Kit, Pierce), following the manufacturer's protocol. Briefly, 2µl of protein lysates were placed in a final volume of 1ml of BCA. Samples were heated for 30min at 37ºC, and then immediately placed in ice to stop the reaction. After 10min, the absorbance was measured and protein concentration was calculated according to the standard curve for the assay.

Immunoblotting:

Protein samples were prepared with 4x LDS sample buffer (Invitrogen) and 1M DTT (to a final concentration of 50mM), and heated at 70ºC for 10min to denaturate the proteins, then the samples were loaded in 4−12% (w/v) Bis−Tris or 3−8% (w/v) Tris−Acetate precast NuPage® SDS-PAGE gels (Invitrogen). The gels were run in NuPage® MES SDS running buffer or NuPage® Tris−Acetate SDS running buffer (Invitrogen) at 90V for 30min and 150V for 1h. Proteins were blotted into PVDF membrane (BioRad) previously activated with methanol, in a Transblot® SD SemiDry Transfer cell (BioRad) at 23V for 1h.

Protein loading on the membranes was visualized using a Red Ponceau solution (0.5% (w/v) Red Ponceau, 1% (v/v) acetic acid). Membranes were washed with a 0.01% (v/v) Tween−Tris−buffered saline solution (TBST) and blocked with 5% (w/v) low fat−milk in TBST for 1h at room temperature. Primary antibody incubation was carried either at room temperature (RT) or at 4ºC when overnight (O.N) depending on the antibody as described in **Table 3**.

Name	Manufacturer	Code	Concentration	Incubation	Secondary Ab. HRP−Conjugated
Actin	Sigma	A4700	1:10000	30min RT	Anti−Mouse
Actin	SantaCruz	SPM161	1:10000	30min RT	Anti−Mouse
Bmal−1	AbCam	ab93806	1:1000	60min RT	Anti−Rabbit
Bmal−1	Novus Biologicals	NB100-2288	1:500	O.N 4ºC	Anti−Rabbit

Table 3. List of antibodies used for western blotting, manufacturer and code. Concentration used and buffer used for dilution (BSA or Milk). Secondary antibody used for each primary antibody, all HRP−conjugated anti IgG (H+L).

Secondary antibodies used were goat anti rabbit (H+L) horseradish peroxidase (HRP) conjugated, and goat anti mouse (H+L) HRP conjugated. Secondary incubation was conducted at a dilution of 1:2000 in 5% (w/v) milk/TBST for 1h at room temperature. Membranes were developed with the enhance chemiluminescence kit (SuperSignal West Pico Chemiluminescent Substrate, Pierce). The chemiluminscence signal from the bands was captured in autoradiographic film (Kodak).

4.6 Histology

4.6.1 Cryosections

Muscles were collected from control and *Bmal1* mKO animals and then immediately frozen in precooled isopentane in liquid nitrogen. Samples were stored at −80ºC until the time of sectioning. Immediately prior to sectioning, muscles were equilibrated to −20ºC, and cut in the cryostat. Serial sections of 8 to 10um thickness were cut and attached to positively charged slides (SuperFrost Plus, ThermoFisher). Slides were kept at −20ºC until use.

4.6.2 Histochemistry

Slides containing control and *Bmal1* mKO muscle sections were subjected to hematoxylin and eosin (H&E) staining, and succinyl dehydrogenase (SDH) staining. These are described in detail below.

Hematoxylin and Eosin (H&E) staining was used to visualize muscle morphology.

Slides were fixed with 4% (w/v) PFA/PBS and washed three times with PBS. They were incubated with hematoxylin for 6min, rinsed in running water for 3min, placed in alcoholic acid (0.3% (v/v) hydrochloridric acid/ ethanol) for 10min, rinsed again in running water for 3min before finally incubating them with Eosin for 1min. The sections were then dehydrated with three steps of increasing concentrations of ethanol (75%, 95% and 100% (v/v)) for 5min each, and then with xylene before mounting with Entellan® (Merk), a resin−embedding medium.

Succinyl dehydrogenase (SDH) Staining

SDH incubation solution:
1mg/ml Nitroblue tetrazolium
0.1M Sodium succinate
0.1M Phosphate buffer

Slides were placed in the SDH incubation solution for 1h at 37ºC, after that they were washed in running water for 2min and mounted with Elvanol (polyvinyl alcohol, Sigma), a hydrophilic mounting medium.

4.6.3 Immunofluorescence

Slides containing control and *Bmal1* mKO muscles were air−dried, and incubated with M.O.M blocking reagent (Vector laboratories) to avoid nonspecific binding of the antibodies. Slides were incubated with primary antibodies against three type of myosin heavy chain listed in **Table 4** (Schiaffino *et al.*, 1989), in 0.5% (w/v) BSA/PBS with 2% (v/v) goat serum for 1h at 37ºC or overnight at 4ºC. The sections were then washed with PBS three times for 5min, followed by an incubation with the fluorophore−conjugated secondary antibody (**Table 4**, made in goat) in a dilution 1:200 in 4% (v/v) goat serum and 0.5% (w/v) BSA in PBS for 1h at room temperature. Slides were washed in PBS, rinsed with water and mounted with Elvanol (Sandonà *et al.*, 2012).

Name	Manufacturer	Code	Concentration	Recognize
Myosin heavy chain I	Developmental Studies Hybridoma Bank (DSHB, University of Iowa)	BA−D5	1:100	
Myosin heavy chain IIB	DSHB, University of Iowa	BF−F3	1:100	
Myosin heavy chain IIA	DSHB, University of Iowa	SC−71	1:50	
Goat anti mouse IgG, Fc_ 2b subclass specific DyLight405	Jackson ImmunoResearch	115−475−207	1:200	BA−D5
Goat anti mouse IgM DyLight549	Jackson ImmunoResearch	115−505−075	1:200	BF−F3
Goat anti mouse IgG, Fc_ 1 subclass specific DyLight488	Jackson ImmunoResearch	115−485−205	1:200	SC−71

Table 4. List of the antibodies used for the myosin – fiber type characterization

Imaging

Images were captured with an epifluorescence microscope coupled with a CCD camera. Different excitation wavelengths and filters were used depending on the fluorophore conjugated to the secondary antibody. The software used for the image acquisition was the Leica Application Suite (LAS).

4.6.4 Electron microscope preparation

Muscles from control and *Bmal1* mKO animals were collected and cut into small pieces. The small muscle pieces were fixed in 2.5% (w/v) glutaraldehyde/ 0.1M sodium cacodylate at 4ºC for 4h. Next, they were subjected to repeated washes in 2% (w/v) sucrose /0.1M sodium cacodylate. Samples were stained with 1% (w/v) OsO_4 /0.1M sodium cacodylate for 2h at 4ºC, then washed with 2% (w/v) sucrose/0.1M cacodylate four times during 90min. After this, samples were subjected to a dehydration process with increasing concentration of ethanol

at 4ºC, 50% (v/v) ethanol for 5min three times, 70% (v/v) ethanol 5min three times, 95% (v/v) ethanol 10min two times and finally absolute ethanol at room temperature for 15min four times. To continue with the dehydration process samples were placed in acetone for 15min twice, keeping them always covered by the liquid.

For the embedding process, the samples were included in an increasing concentration of the Epoxy−embedding medium (resin), starting with acetone/resin 2:1 for 30min at room temperature, acetone/resin 1:2 for three hours and overnight with the resin allowing it to penetrate the muscle pieces. The following day the samples are placed in a sample cast adding fresh resin and placing the cast at 70ºC for approximately three days so the epoxy−embedding medium can polymerize.

In order to have an idea of the quality of the embedding of the samples and to choose the areas of interest semi−thin, 1µm thick, sections were cut in the utramicrotome then placed in slides and stained with toluidine blue, once the right orientation was found it was possible to continue with the thin sections. Thin longitudinal and transverse sections, 70nm thick, were cut for the following electron microscopic analysis. Samples were collected in copper grids and contrasted with uranyl acetate for 20min followed by washes with water and incubation with lead citrate for 5min and rinsed with water.

Imaging

Images from control and *Bmal1* mKO muscles were taken with Tecnai 12 (FEI) Transmission electron microscope (TEM) coupled to a CCD camera, and using the TIETZ software.

4.7 *In vivo* muscle force measurements

Mice were anaesthetized with a mix of 2% Xylazine® (Bio 98 S.r.l) and Zoletil® 100 (Virbac). The sciatic nerve was exposed and electrode wires were implanted on both sides of the nerve and the common peroneal nerve was dissected. Then the animals were sutured and placed on a table where the foot

was fixed to a footplate connected to a muscle lever system (Model 305C; Aurora Scientific). Force frequency curves were determined by stimulating the sciatic nerve with increasing frequency pausing for 30sec after each stimulus to avoid fatigue (Blaauw *et al.,* 2008; Blaauw *et al.,* 2009).

4.8 Statistical analysis

All data are presented as mean ± S.E.M. Data were analyzed with Student's t−tests. Statistical significance was accepted at p−values <0.05.

5 RESULTS

5.1 *Bmal1*$^{fl/fl}$ x *MLC1f*−Cre mice

5.1.1 Characterization of the animal model

In order to investigate the function of the clock gene *Bmal1* in skeletal muscle, we generated conditional *Bmal1* muscle−specific knockout mice (*Bmal1* mKO) by crossing the *Bmal1*$^{fl/fl}$ mice line with the *MLC1f*−Cre line. Mice homozygous for the floxed *Bmal1* allele and heterozygous for Cre were used as the experimental group, whereas their Cre negative littermates were used as controls. First, the genotype of each mouse was established by standard PCR of genomic DNA (**Figure 5**A). Next, RT−qPCR confirmed the specificity of the knockdown of Bmal1 exclusively in skeletal muscle in tissue samples from soleus (SOL), tibialis anterior (TA) and heart. Whereas in control skeletal muscle *Bmal1* mRNA expression followed an oscillatory expression across the day/night cycle, in *Bmal1* mKO mice *Bmal1* mRNA was drastically reduced and did not maintain its oscillatory pattern (**Figure 5**B). Similarly, BMAL1 protein levels were also reduced, as confirmed by western blot analysis of gastrocnemius (GA) muscle lysates from control and *Bmal1* mKO mice. In these samples a band of approximately 60KDa was evident in the control and absent in Bmal1mKO mice (**Figure 5**C). These first results confirmed the successful ablation of BMAL1 selectively in skeletal muscle, which allowed us to proceed to characterization of the phenotype.

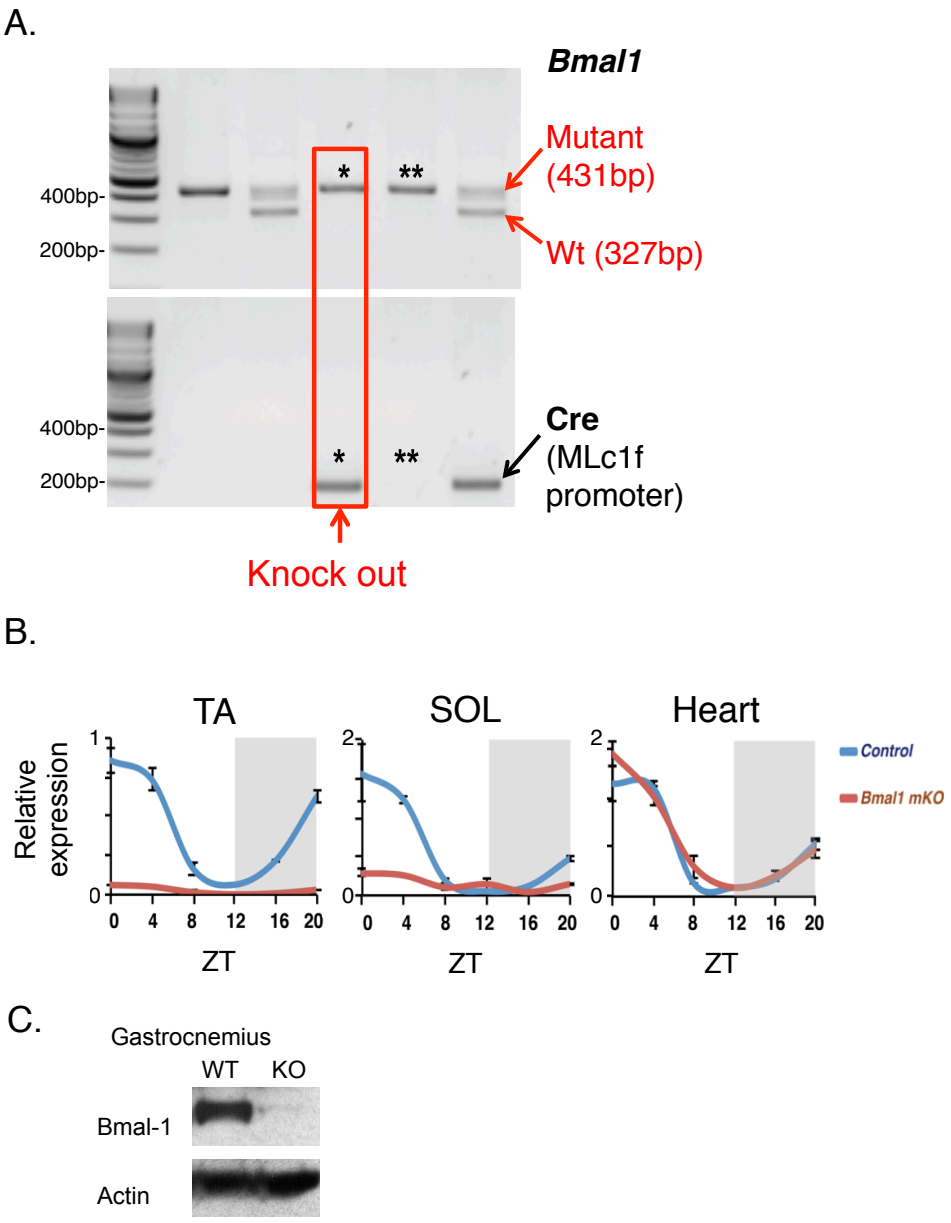

Figure 5. Preliminary characterization of the mouse model with disrupted clock gene *Bmal1*. **A**. PCR product for *Bmal1* and Cre, *Bmal1* 431bp band contains the two LoxP sites; Animals with the mutant band for *Bmal1* and with the band for Cre are the KOs (*) and controls carry the mutated allele (**). **B**. RT−qPCR for the *Bmal1* transcript, (corrected for the housekeeping gene *36B4)*. Showing temporal profile of *Bmal1* transcript in slow SOL, fast TA and cardiac muscle at Zeitgeber times (ZT0 = lights on, ZT12 = lights off). Note the specificity of the *Bmal1* excision in skeletal muscle and not in cardiac muscle of *Bmal1* mKO. **C**. Loss of BMAL1 protein in GA demonstrated by western blot at Zeitgeber time 4 with an anti−BMAL1 antibody (AbCam), normalized with panactin (Sigma)

5.1.3 *Bmal1* mKO phenotype

Initial observations showed that *Bmal1* mKO mice reproduce normally, and do not present any gross differences in appearance when compared to their control littermates. *Bmal1* mKO showed a normal growth (**Figure 6**A) and lifespan (**Figure 6**B). This is in stark contrast with whole body *Bmal1* KO mice, which were reported to have severely impaired survival and growth, with significant reductions in both muscle mass and fiber size. Surprisingly, muscle mass increased by ~15% in fast TA and GA muscles from *Bmal1* mKO compared to control littermates (**Figure 6**C), and an ~8% increase in fiber size was also observed in TA (**Figure 6**D).

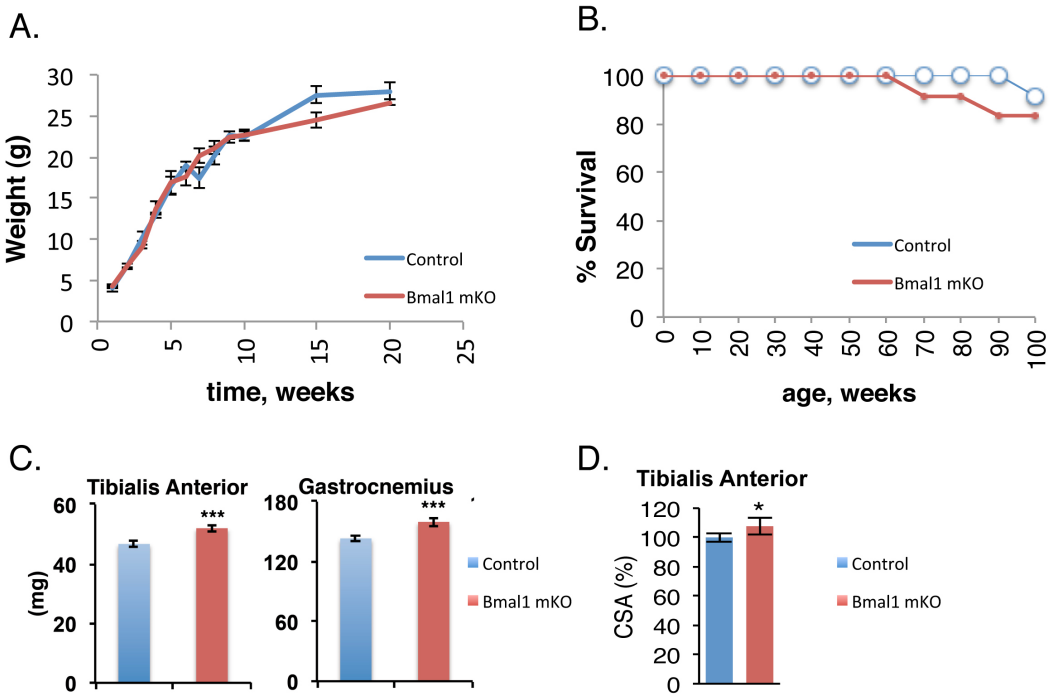

Figure 6. Time course of growt and lifespan of control (blue) and *Bmal1* mKO (red) mice. **A**. Mean body weight (g) measured until adult age. **B**. Lifespan curve, note the survival of the *Bmal1* mKO compared to wild type littermates. **C**. Muscle weight (mg), comparison of tibialis anterior, and gastrocnemius, increased muscle mass in the *Bmal1* mKO. **D**. Cross−sectional area of the tibialis anterior relative to control (Significance: * $p<0.05$ *** $p<0.01$, Student's t−test).

To investigate the role of BMAL1 in muscle morphology, we performed histological examination of tibialis anterior (TA) muscle cryosections. We stained with hematoxylin and eosin to discern signs of histological changes, and with SDH staining to have a preliminary assessment of fiber type composition and distribution (oxidative vs. glycolytic). The comparison between control and *Bmal1* mKO muscles revealed a normal structure without any signs of tissue alteration (**Figure 7**A) and a similar distribution of oxidative and glycolytic fibers (**Figure 7**B).

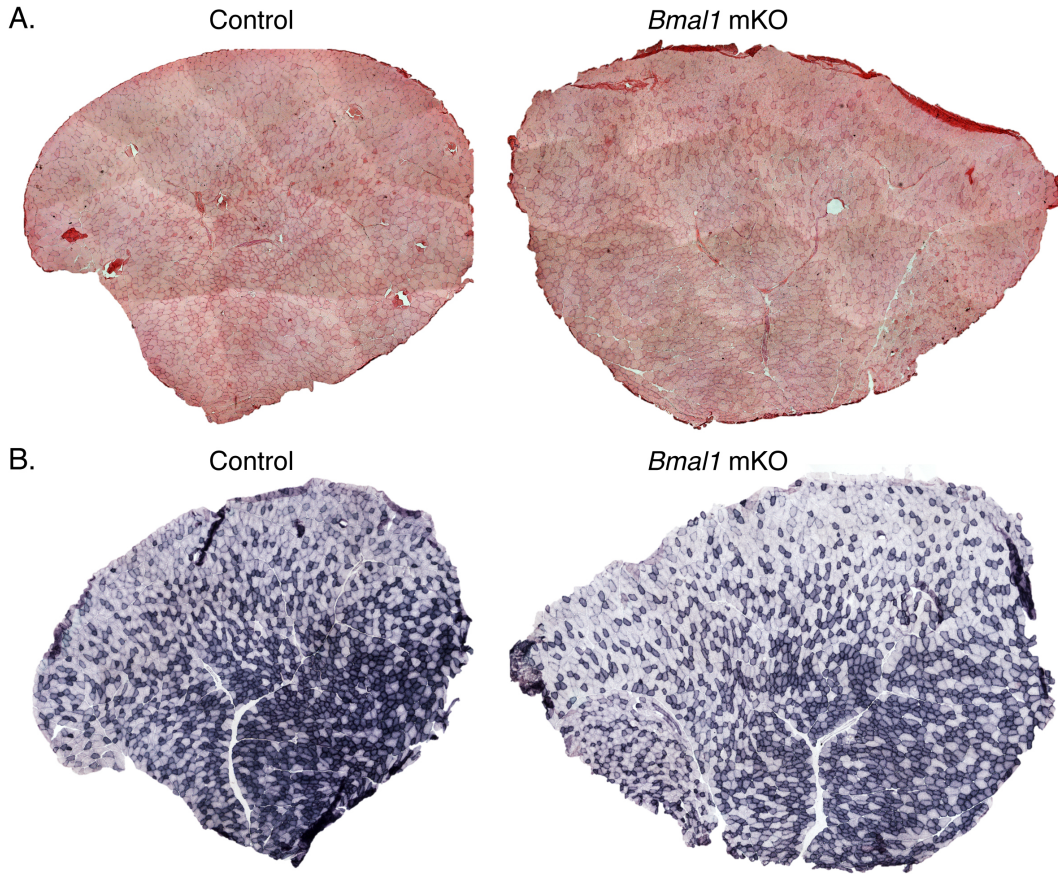

Figure 7. Histological analysis of the TA muscles from Control and *Bmal1* mKO mice. Cross−section of the TA stained with **A**. Hematoxylin Eosin (H&E) staining. **B**. Succinate dehydrogenase staining (SDH). Note normal structure and similar distribution of oxidative and glycolytic fibers.

In control mice electron microscopy reveals normal myofibrillar architecture with regular hexagonal distribution of thin and thick filaments, and correct alignment of the sarcomeres important for a precise muscle function. In *Bmal1*$^{-/-}$ mice this muscle structure was reported to be severely disrupted (Andrews *et al.*, 2010). However, in the *Bmal1* mKO muscles, there was no alteration in the organization of the thin and thick filaments (**Figure 8**A) or in sarcomere alignment (**Figure 8**B).

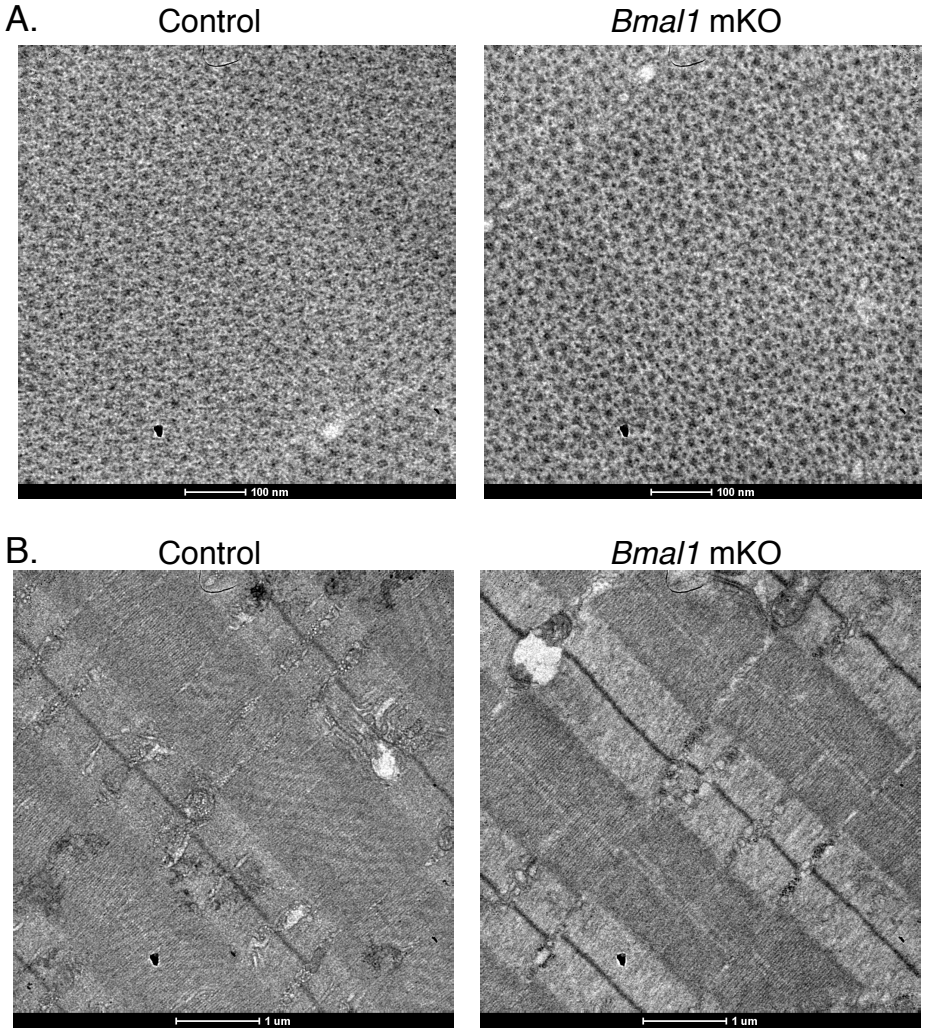

Figure 8. Myofibrillar architecture visualized by transmission electron microscopy. **A.** Transversal image, normal alignment of thin and thick filaments. **B**. Longitudinal image of the sarcomere organization, see normal disposition of the sarcomere

Skeletal muscle is composed of different types of muscle fibers that can be classified according to their predominant myosin heavy chain and its shortening velocity: type 1 slow, type 2A moderately fast, type 2X fast and type 2B highly fast fibers (Schiaffino, 2010). In order to determine whether fiber type composition is changed in *Bmal1* mKO muscles, cross−sections of soleus (SOL) and extensor digitorium longus (EDL) muscles from 5−month−old control and Bmal1mKO were stained for myosin heavy chain I, IIA and IIB, and quantifying the number of fibers stained for each myosin (**Figure 9**A), *Bmal1* mKO SOL showed a decrease in slow type 1 fibers ($p<0.05$) accompanied with an increase in 2A−type fibers ($p<0.05$) (**Figure 9**B upper panel), whereas the EDL showed decrease type 2X fibers ($p<0.05$) with a tendency towards an increase in type 2B fibers (**Figure 9**B lower panel).

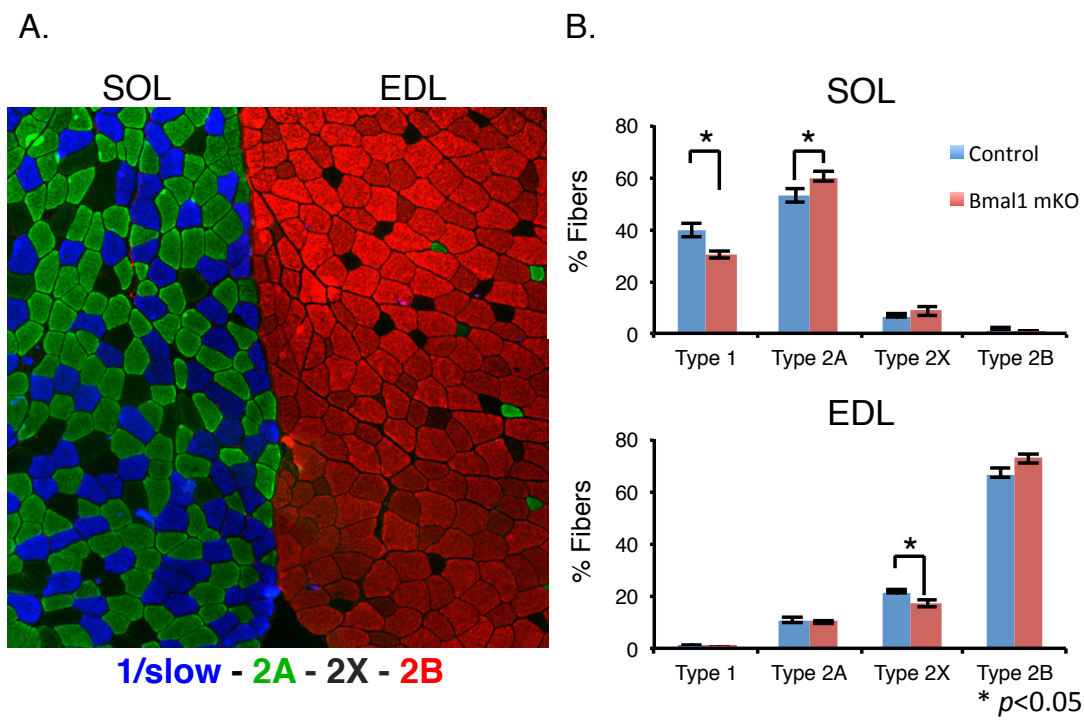

Figure 9. Fiber−type composition. **A**. Representative cross−section of the slow soleus (SOL) and the fast extensor digitorium longus (EDL) muscles in *Bmal1* mKO immunostained for myosin type I (blue), type IIA (green), type IIB (red), and type IIX (black/ unstained) fibers. **B**. Quantification of the fiber types; upper panel SOL fiber type composition, lower panel EDL fiber type composition note a significant switch towards faster type of fibers (*$p<0.05$, Student's t−test)

5.1.4 Locomotor activity

Mice are nocturnal, and as such are active at night. Considering that in *Bmal1* knockout mice circadian rhythms of locomotor activity were found completely disrupted (Bunger *et al*., 2000), we wondered whether the local disruption of *Bmal1* exclusively in skeletal muscle would lead to similar changes in circadian locomotor activity. Our results showed that the circadian rhythm of activity in the *Bmal1* mKO mice was normal, with a clear increase in activity during the dark phase (**Figure 10**). While activity rhythm was normal, a significant (~20%) increase in activity during the dark phase was observed in *Bmal1* mKO mice compared to their control littermates.

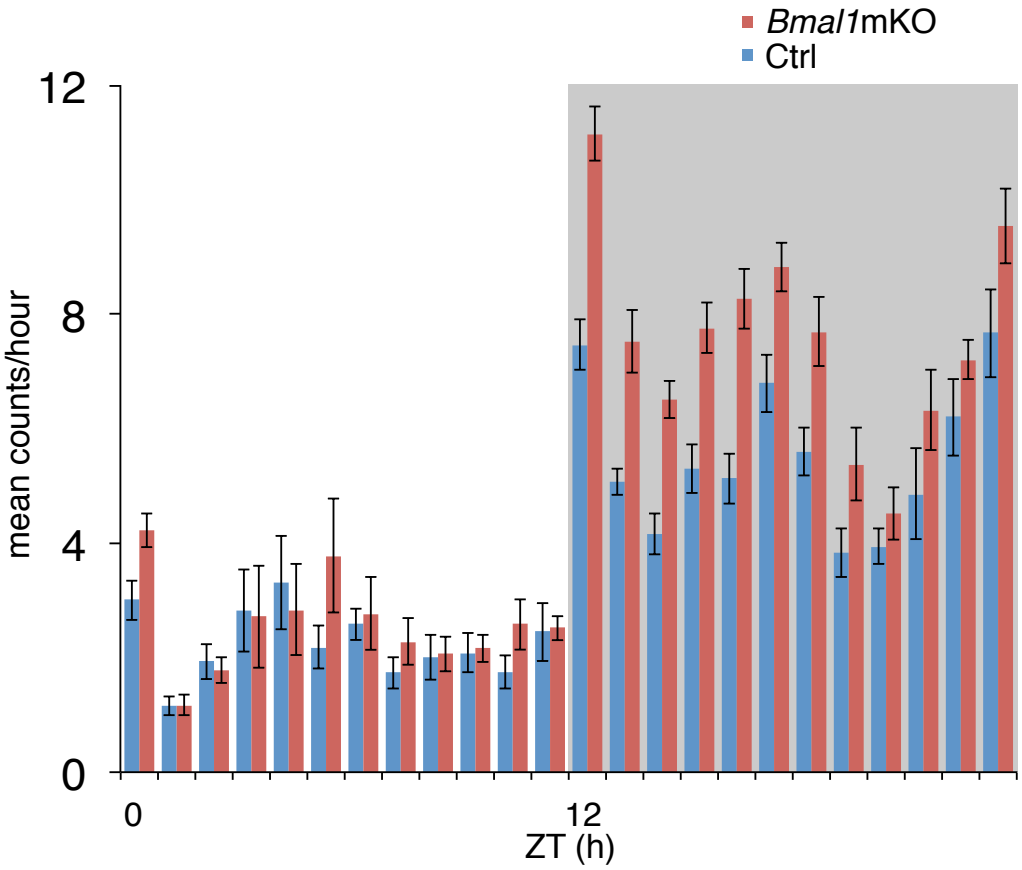

Figure 10. Locomotor activity was monitored by biotelemetry sensors implanted in the peritoneum, measuring the free movements of the animals in the cage. Red bars show *Bmal1* mKO, blue bars control animals

5.1.6 Force measurements

We measured the muscle force by stimulating the gastrocnemius muscle in anaesthetized mice to investigate whether the ablation of *Bmal1* is accompanied by a loss in muscle strength, as was the case in the *Bmal1* knockout mice, both at the level of the whole muscle and single fibers (Kondratov *et al*., 2006; Andrews *et al*., 2010). Comparing the two groups (control and *Bmal1* mKO) the absolute force is decreased by 12% in the *Bmal1* mKO. When the values of the absolute force are normalized by the muscle weight, the difference between control and *Bmal1* mKO is manifested in a 20% decrease in maximum force production (**Figure 11**).

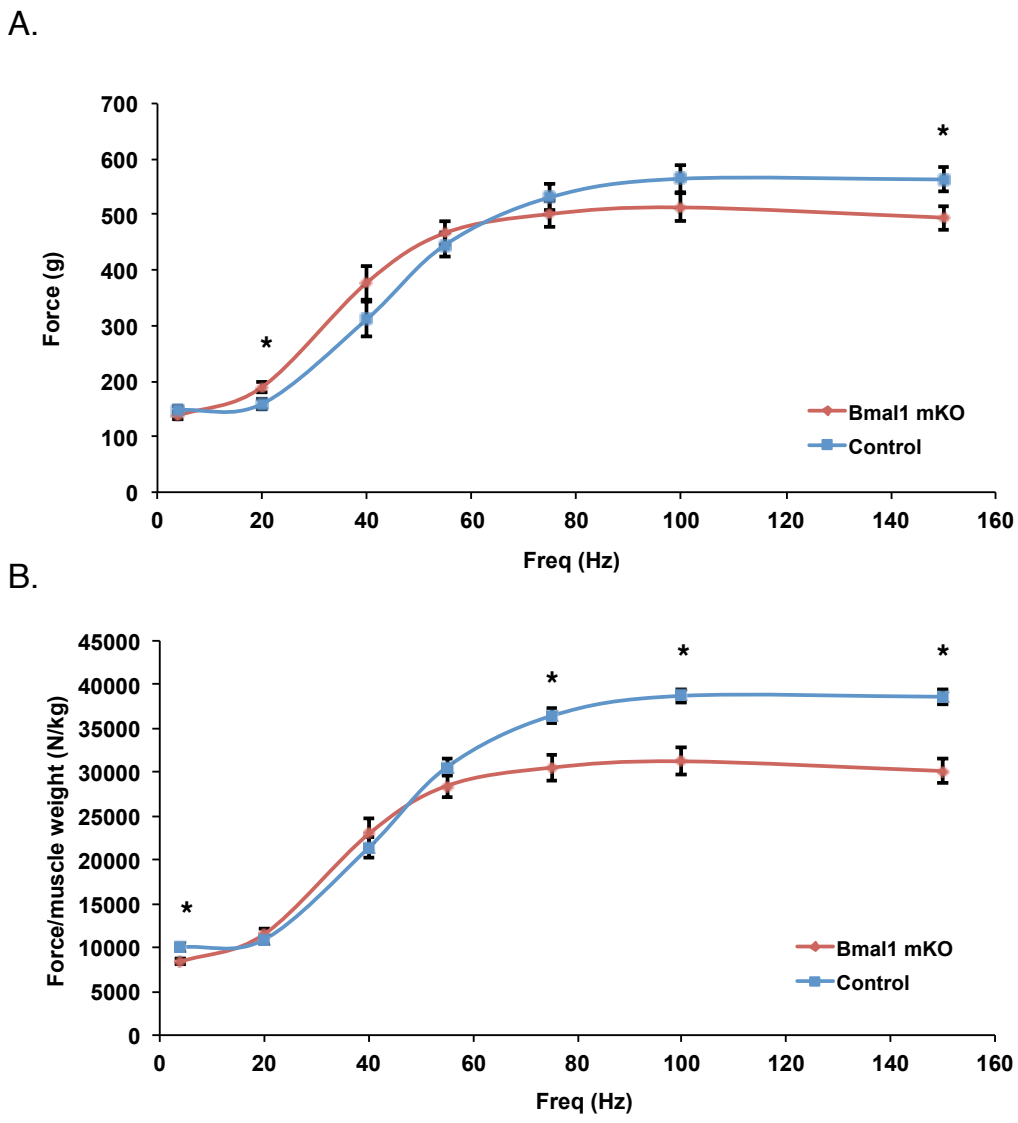

Figure 11. Force measurements: Stimulation of the Gastrocnemius muscle in *Bmal1* mKO and controls. **A**. Absolute force (force: g, frequency of the stimulus: Hz). **B**. Normalized force by body weight (N/Kg, Hz) (*p<0.05 Student's t−test).

5.2 Gene expression profile

The transcription factor BMAL1 is a crucial component of the molecular clock that keeps tissue−specific gene expression entrained to the 24h day/night cycle. We therefore wanted to investigate the effect on muscle specific *Bmal1* knockout on the skeletal muscle circadian transcriptome. Microarray analyses were performed in fast TA and slow SOL muscles collected every four hours over a total of 24h (Zeitgeber times 0, 4, 8, 12, 16 and 20). The JTK_CYCLE algorithm (Hughes *et al.,* 2010) was used to identify genes which cycle within this 24h period. A comparison of control fast and slow muscles identified 684 cycling genes in control fast TA and 1359 cycling genes in control slow SOL muscle. In the absence of the clock gene *Bmal1* only 197 genes maintained their circadian oscillation in *Bmal1* mKO TA, whereas only 693 genes continued to cycle in Bmal1 mKO SOL (**Table 5** and **Figure 12**A). These genes would be likely regulated by circadian systemic factors, which continue cycling in the absence of a functional muscle clock.

Muscle	Cycling genes in control muscles	Genes still cycling in *Bmal1* mKO muscles	Genes no longer cycling in *Bmal1* mKO muscles
TA muscle	684	197	487
SOL muscle	1359	693	666

Table 5. Cycling genes identified by JTK_CYCLE algorithm in muscles from control and *Bmal1* mKO (BH Q−value< 0.2)

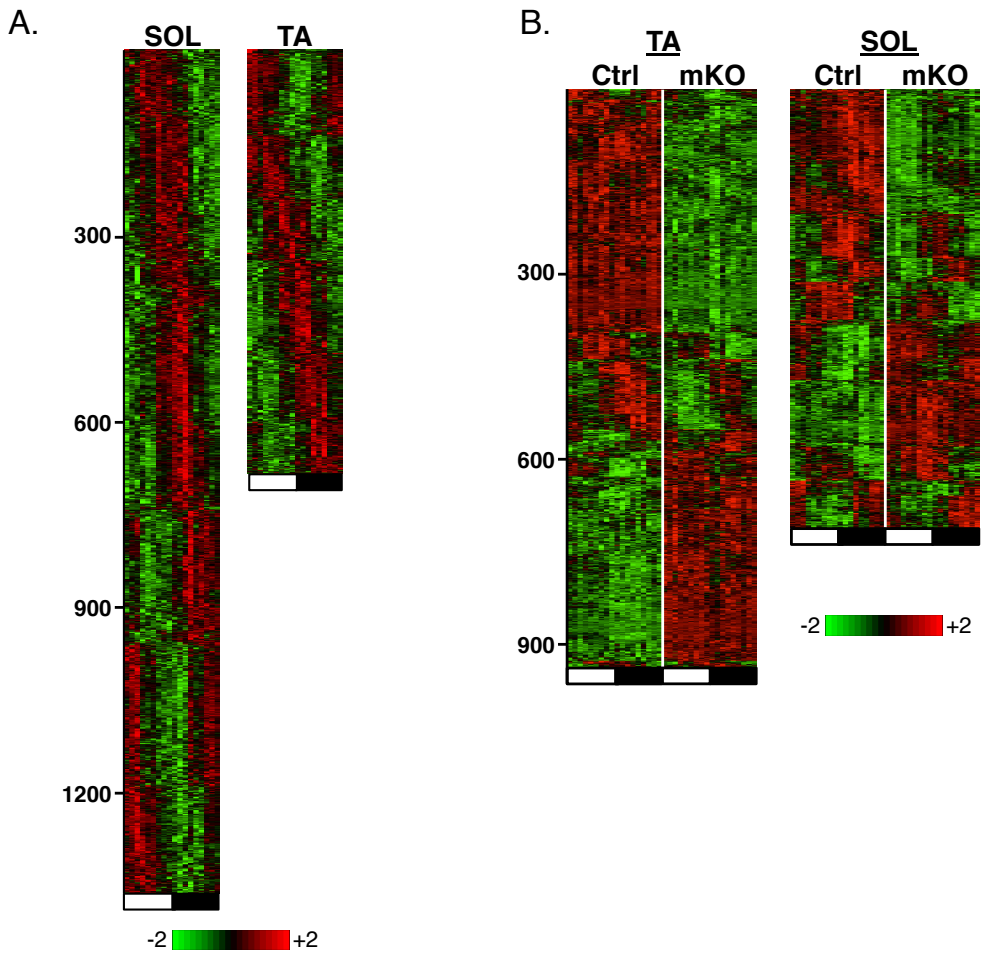

Figure 12. Gene expression profile. **A**. Phase map of circadian transcripts in control SOL and TA muscles identified using JTK_CYCLE (BH Q−value <0.2). **B**. Phase map of the differentially expressed genes identified using magSigPro algorithm TA (fast muscle) and SOL (slow muscle) in green down−regulated genes and red up−regulated genes. Muscles were collected at 4h intervals through the day (white box) and night (dark box)

Using the magSigPro method (Conesa *et al.,* 2006) 931 genes were differentially expressed in TA and 706 genes in SOL muscle (**Figure 12**B).

We were able to validate the results of the microarray by performing RT−qPCR on selected genes. As previously demonstrated in **Figure 1**C, the *Bmal1* transcript follows a circadian pattern of expression in control TA muscle that is completely abrogated in *Bmal1* mKO (**Figure 13**).

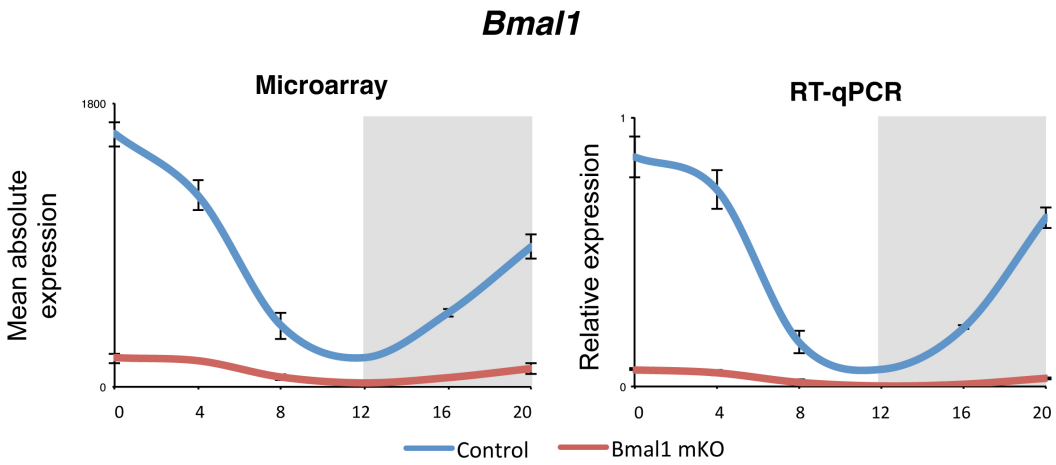

Figure 13. Microarray analysis of *Bmal1* gene (mean±SEM; n=3/time point), was validated by qPCR and plotted relative to *36B4* expression (±SEM; arbitrary units; n=3/time point) in TA muscles

As expected, genes previously known to be part of the core clock machinery showed a markedly altered expression between control and *Bmal1* mKO muscles. For example the *Period* genes, directly transcriptional targets of the CLOCK:BMAL1 complex showed a decrease in transcript levels. Specially, *Per1* and *Per3* were decreased, but *Per2* was only slightly disturbed. The oscillatory pattern of *Cryptochrome* genes, also transcriptional targets of CLOCK:BMAL1, was abolished for *Cry2* although the levels of *Cry1* were increased. *Clock* also showed increased mRNA levels (**Figure 14**).

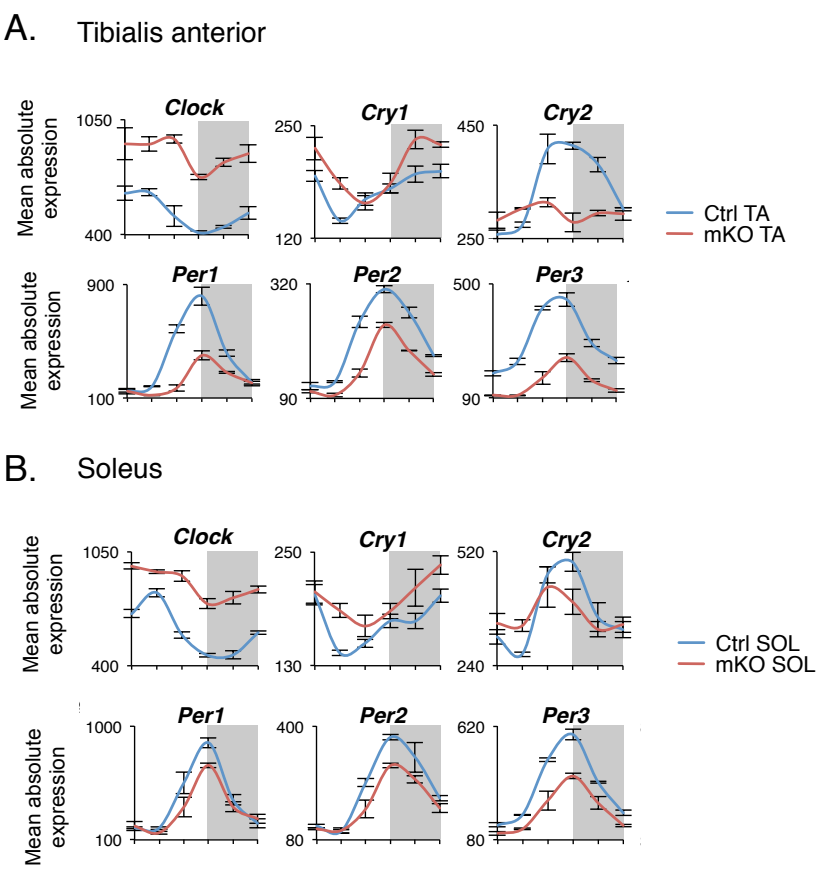

Figure 14. Transcript levels of core clock genes in **A**. TA muscle and **B**. SOL muscle. Gene expression was determined by microarray analysis from samples taken every four hours during a day (mean ±SEM; n=3 per time point)

Additional target genes of the CLOCK:BMAL1 complex, such as *Rev−Erbα*, PAR family members *Dbp*, *Tef*, and *Hlf*, all showed a marked decrease (**Figure 15**), whereas *E4bp4/Nfil3,* a negative regulator of the BMAL1−dependent expression, was increased (**Figure 15**).

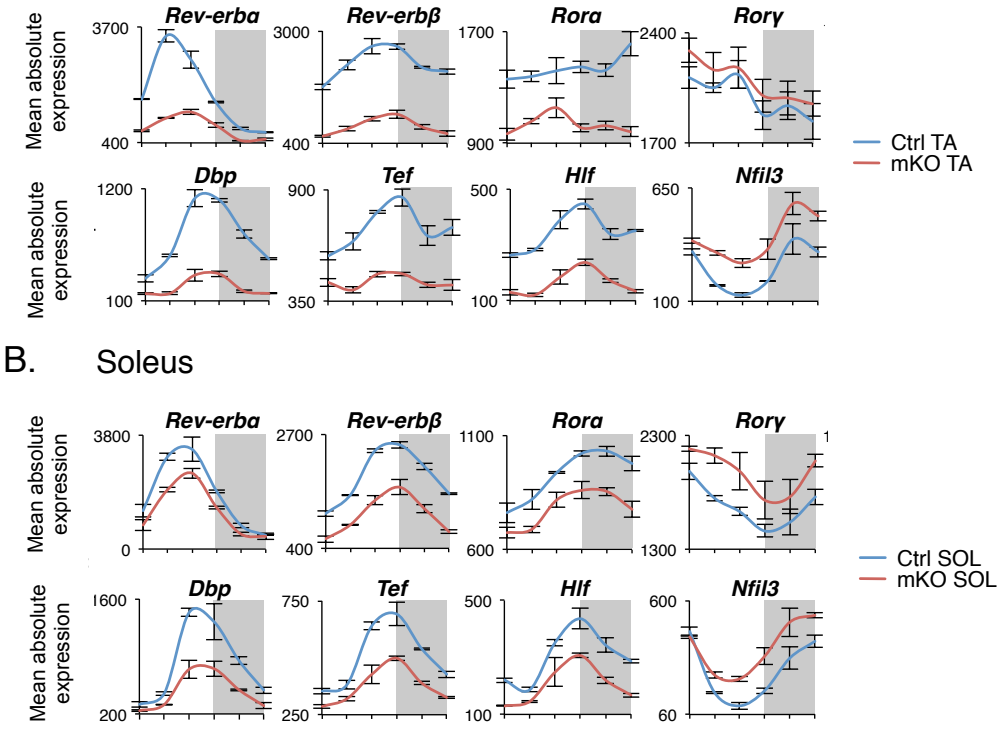

Figure 15. Transcript levels of clock associated genes part of secondary loops of regulation in **A.** TA muscle and **B**. SOL muscle. Gene expression was determined by microarray analysis from samples taken every four hours during a cycle of 24h (mean ±SEM; n=3 per time point)

Some genes that lost their rhythmicity in *Bmal1* mKO muscles have defined physiological roles in muscle function. For example, *Acvr1b* encodes for the activin receptor 1b, part of the myostatin receptor complex, or *Asb2* codes for an E3 ubiquitin ligase expressed in skeletal muscle (**Figure 16**A). In the *Bmal1* mKO muscles, cycling *Acvr1b* was strongly reduced, and expression levels remain lower than basal levels in the control muscle. On the other hand, *Asb2* levels remain constitutively high, corresponding to the peak levels of control muscles.

While some genes lost their oscillatory pattern, it was observed that certain other genes maintained their circadian expression. For example: *FoxO1*, which encodes for a transcription factor important in the regulation of muscle mass, shows an identical pattern of expression in *Bmal1* mKO muscles (**Figure 16**B).

Other genes were only slightly affected, such as *Fbxo32*, which encodes the muscle−specific E3 ubiquitin ligase atrogin1/MAFbx and displays a phase−shift of about 4h phase delay in *Bmal1*mKO (**Figure 16**B).

Other genes maintained cyclic expression, but with altered levels of expression having either increased levels of expression. For example, *Myod1* (**Figure 16**B), a myogenic regulatory factor that has been identified as a circadian gene (McCarthy *et al.,* 2007) was increased but maintained its temporal profile. Alternatively, Ky (**Figure 16**B), a Z−disk associated protein−coding gene (Baker *et al.,* 2010), was shown to be down−regulated in *Bmal1* mKO muscles.

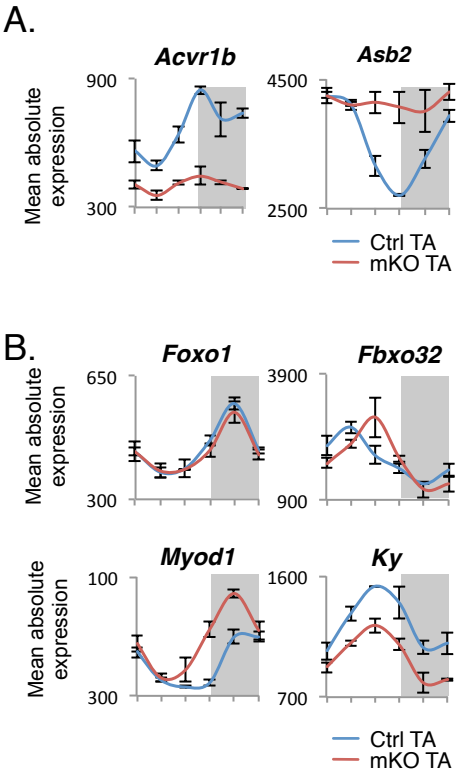

Figure 16. Transcript levels of cyclic genes. **A**. Cyclic genes that show an ablation of the oscillatory pattern in the *Bmal1* mKO. **B**. Cyclic genes that keep the normal oscillatory pattern in *Bmal1* mKO, or show phase shift or increased/decreased levels

5.2.1 Altered pathways

In order to identify biologically meaningful changes that occur in *Bmal1* mKO muscles, Gene set enrichment analysis (GSEA) was performed. First the data was analyzed using gene sets from the TRANSFAC database, which groups genes

according to the presence of validated transcription factor binding motifs in their promoter region. Serving as a validation of our approach, it was interesting to note that the top ranking gene sets down−regulated were those under the regulation of E4BP4 and HLF, both output regulators of the clock machinery (**Table 6**, $p<0.01$).

NAME	NOM p−value	FDR q−value
V$E4BP4_01 (NFIL3)	0	9.90E−04
V$HLF_01	1.99E−04	0.001543765
V$CREBP1_01 (ATF2)	0	0.001834922

Table 6. Top three significantly TRANSFAC gene sets enriched in control vs. *Bmal1* mKO and shown to be down−regulated in *Bmal1* mKO muscles. $p<0.05$, False discovery rate (FDD) $q<0.25$. *Bmal1* mKO muscles

Using gene sets from the Biocarta database, which groups genes together based on their presence in a common signaling pathway (**Table 7**), GSEA analysis highlighted a number of significantly enriched pathways that were altered in muscles from *Bmal1* mKO mice compared to controls. In particular, the p38 pathway was enriched in control muscles, suggesting decreased activity in *Bmal1* mKO muscles ($p<0.05$).

Cross−referencing the top ranking gene sets from the analysis using TRANSFAC gene set as reference, we noticed that CREBP1, also known as ATF2, was ranked among the top gene sets enriched in control muscle (**Table 6**). ATF2 is an immediate downstream effector of p38 MAPK pathway. Thus, also suggesting decreased activity of the p38 pathway in *Bmal1* mKO muscles ($p<0.01$). The p38 pathway is a signaling cascade activated by different stimuli such as stress or exercise; ATF2 is a chromatin regulator, which binds to c−AMP responsive elements in response to signals from the p38 MAPK and JNK pathway.

NAME	NOM *p*−value	FDR *q*−value
NTHI_PATHWAY (NF−kB, downstream of p38MAPK)	3.99E−04	0.048723523
P38MAPK_PATHWAY	0.012185378	0.17000613
HDAC_PATHWAY	0.004636162	0.17391846
CARM_ER_PATHWAY	0.020477137	0.18074787
IL12_PATHWAY	0.00318408	0.18827936
TGFB_PATHWAY	0.024860779	0.2003742
TEL_PATHWAY	0.011890606	0.2154802
LAIR_PATHWAY	0.029792238	0.22962427
SPPA_PATHWAY	0.025768086	0.23862484

Table 7. Pathways down−regulated in *Bmal1* mKO. False discovery rate (FDR) $q<0.25$

We subsequently performed Leading Edge Analysis to identify genes that are common among multiple gene sets, and thus more likely to be of interest. The *Map2K6* gene, which encodes for MKK6, the upstream activator of the p38 pathway, was identified in 12 different data sets as a down−regulated gene in *Bmal1* mKO muscles (**Figure 17**), seen in both TA and SOL muscles (**Figure 18**). From these results we observed that both upstream activators and downstream effectors or targets of this pathway are altered in the *Bmal1* mKO.

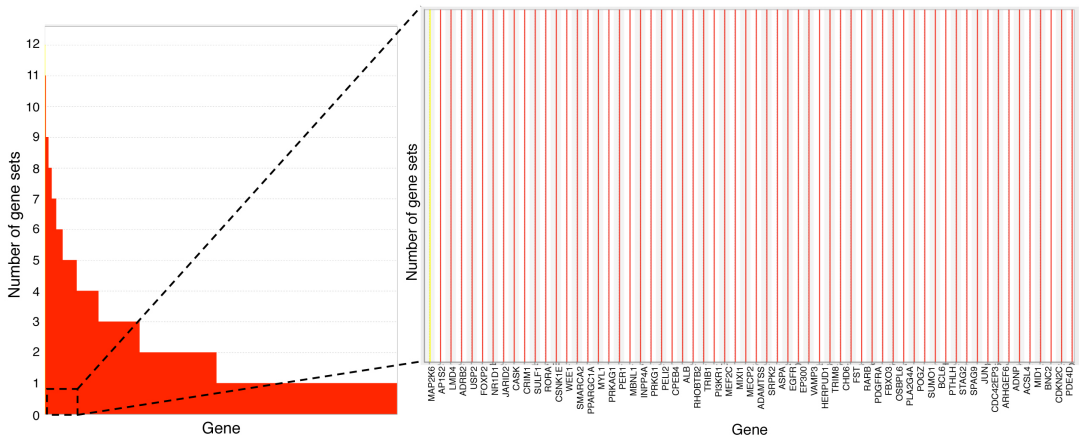

Figure 17. Leading edge analysis. A. Down−regulated genes present in different data sets. B. Zoom in of the list of common genes down−regulated, note *Map2k6* at the top

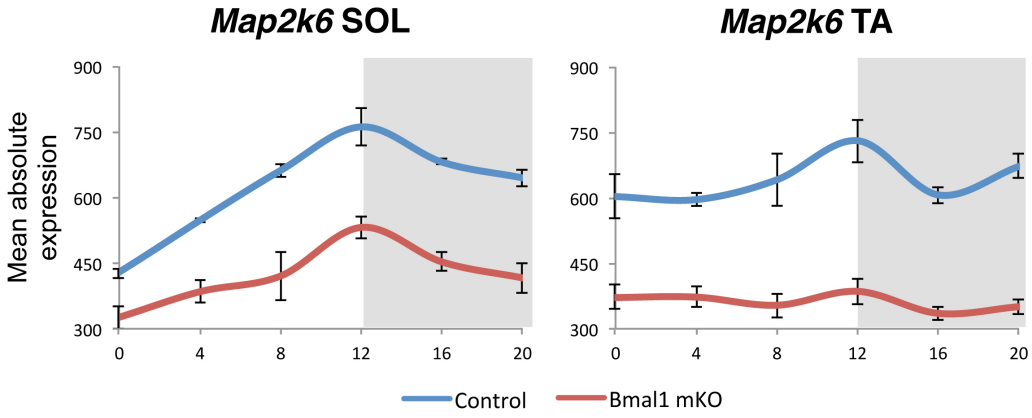

Figure 18. Transcript levels of *Map2K6*, which encodes for MKK6 protein, at different Zeitgeber time points. Note reduced mRNA levels in both TA and SOL from *Bmal1* mKO ($p<0.001$)

5.3 *Bmal1*$^{fl/fl}$ x *HSA*−Cre (Inducible knockout)

The previously described *Bmal1* mKO model had a constitutive lack of *Bmal1* in the muscle from early postnatal stages. In order to elucidate the role of *Bmal1* in adult muscle we generated an inducible muscle−specific *Bmal1* (*Bmal1* imKO), by crossing the *Bmal1*$^{fl/fl}$ line with the tamoxifen inducible *HSA*−CreER line (**Figure 4**B). Both 2−month−old control and *Bmal1* imKO were treated with tamoxifen for 5 consecutive days to induced the Cre−LoxP system.

5.3.1 Preliminary characterization

In line with our previous characterization of the *Bmal1* mKO, we confirmed that the *Bmal1*$^{fl/fl}$ x *HSA*_Cre line was carrying the *Bmal1* mutant allele (431bp) and the Cre allele (200bp) by standard PCR (**Figure 19**A). Then after activation of the Cre activity with the tamoxifen treatment (Schuler *et al.,* 2005), the genomic excision of the *Bmal1* gene in skeletal muscle was confirmed by looking at the transcript levels of *Bmal1* in skeletal muscle at different time points. *Bmal1* mRNA was abolished in the *Bmal1* imKO (**Figure 19**B): the circadian oscillation of the transcript disappeared. The final validation was at the protein level, where BMAL1 was detected to be depleted in the muscles of the induced knockout (**Figure 19**C).

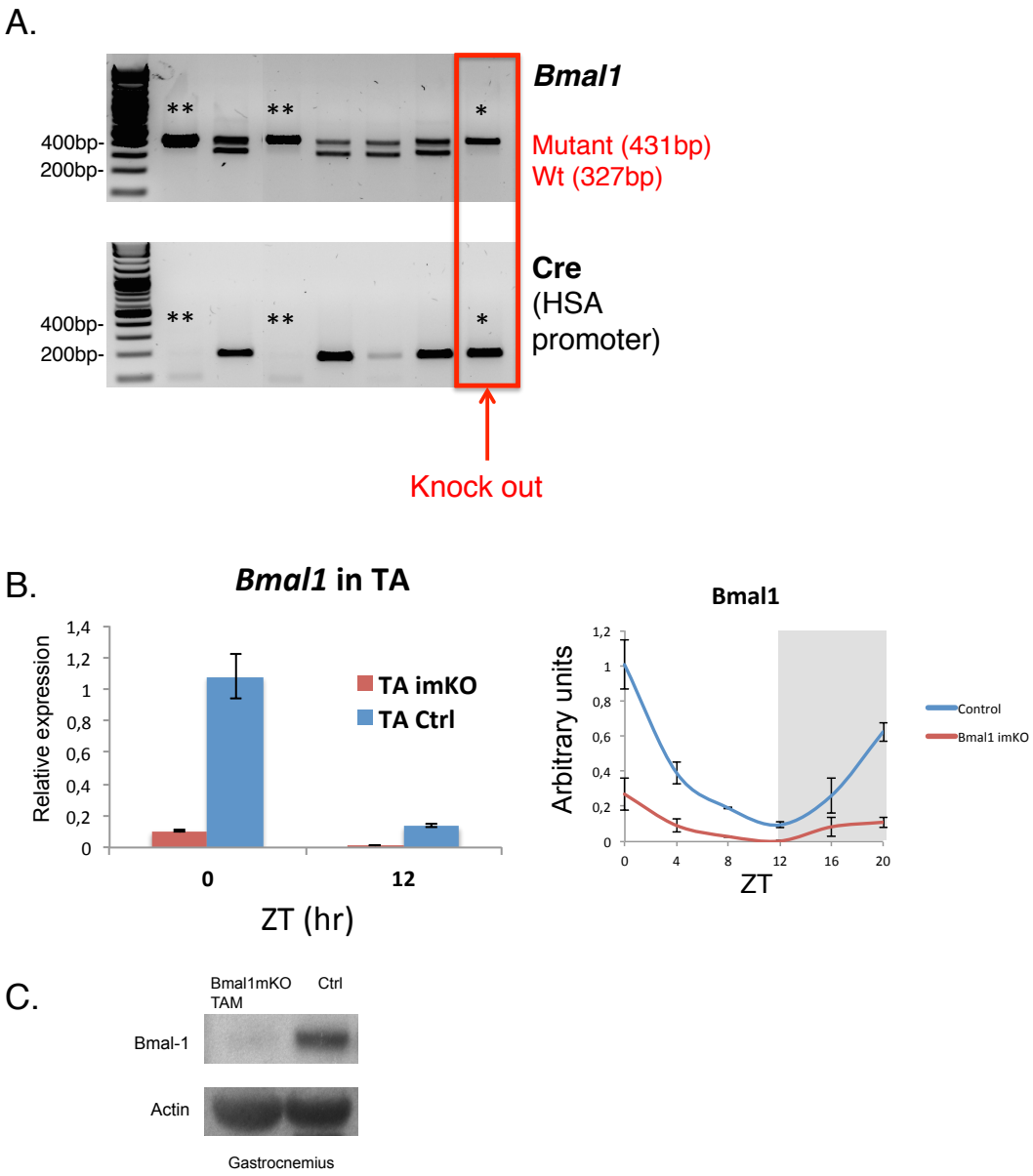

Figure 19. Validation of the animal model. **A.** PCR for *Bmal1* and Cre, *Bmal1* 431bp band contains the two LoxP site; Animals with the mutant band for *Bmal1* and with the band for Cre are the inducible KOs (*), and those without the Cre are controls (**). Animals were treated with tamoxifen and muscles were analyzed one month after the induction of the KO. **B.** RT−qPCR for the *Bmal1* transcript, relative to housekeeping 36B4 gene. Left panel: average value for each group at Zeitgeber times 0 and 12 (three samples per group), Right panel: temporal profile of *Bmal1*. **C.** Western blot for BMAL1 (Novus Biologicals) normalized with panactin

5.3.2 Lifespan, body weight and muscle weight

Animals from this mouse line were allowed to develop as wild type animals and during adulthood the genomic excision of *Bmal1* was induced with 5−day tamoxifen treatment, and no changes in their lifespan were observed. There was

no difference in growth either before or after induction of the knockout (**Figure 20**A and **Figure 20**B, respectively).

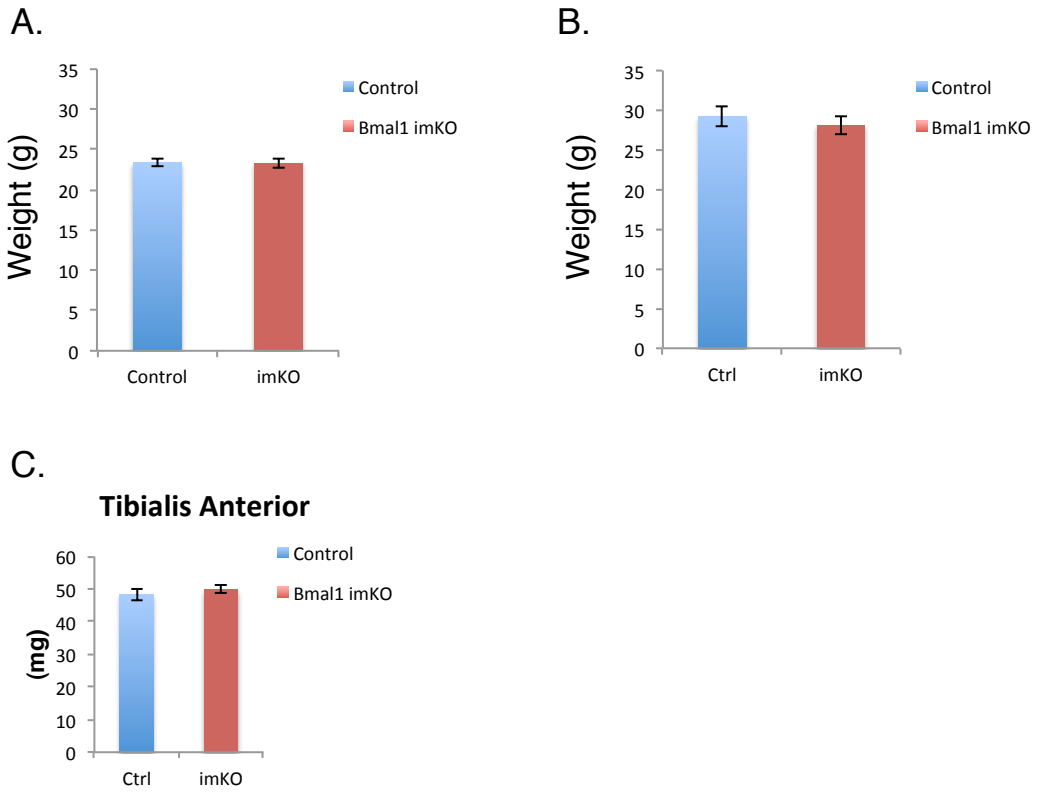

Figure 20. Growth of the *Bmal1* imKO model. **A**. Body weight before induction with tamoxifen. **B**. Body weight at the time of sacrifice, 40 days after tamoxifen−induced knockout. **C**. Muscle weight.

5.3.3 Circadian rhythms of locomotor activity

We questioned whether a sudden ablation of the BMAL1 transcription factor would alter the muscle and so its activity; it was observed that *Bmal1* imKO showed a normal rhythm of locomotor activity during the day, being more abundant during the subjective night (**Figure 21**).

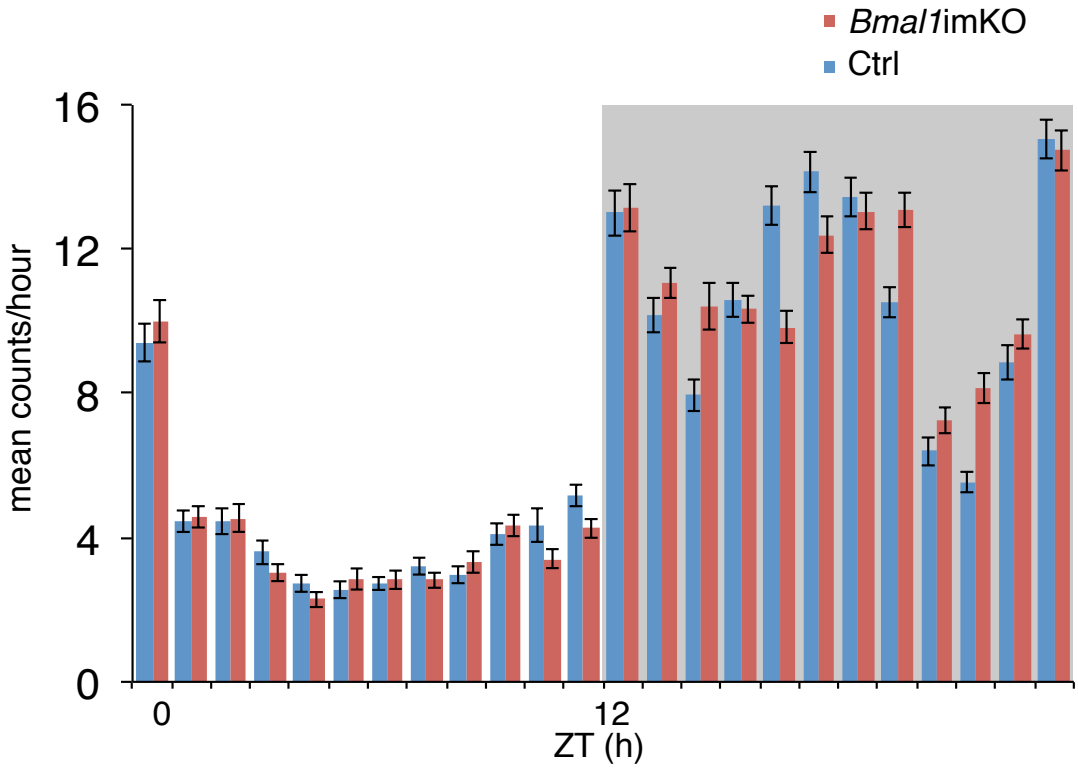

Figure 21. Locomotor activity was monitored by implanted sensors in the peritoneum, measuring the free movements of the animals in the cage. Red bars show *Bmal1* imKO after tamoxifen induction, blue bars control animals

5.3.4 Force measurements

The next step after the induction of the knockout was to determine if the muscle physiological behavior was impaired as was previously shown the *Bmal1* mKO. Our preliminary results did not show significant changes in the force of the *Bmal1* imKO animals (p>0.05) (**Figure 22**).

A.

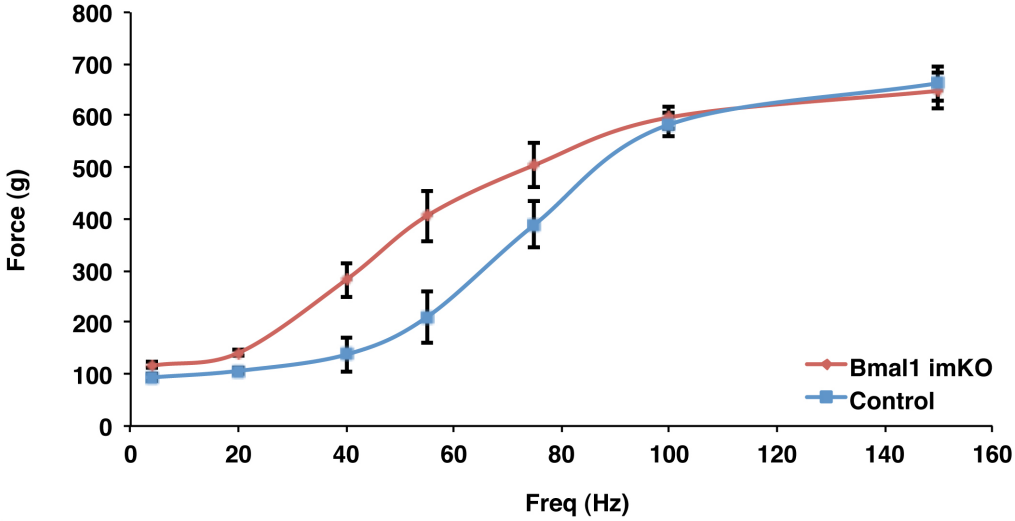

B.

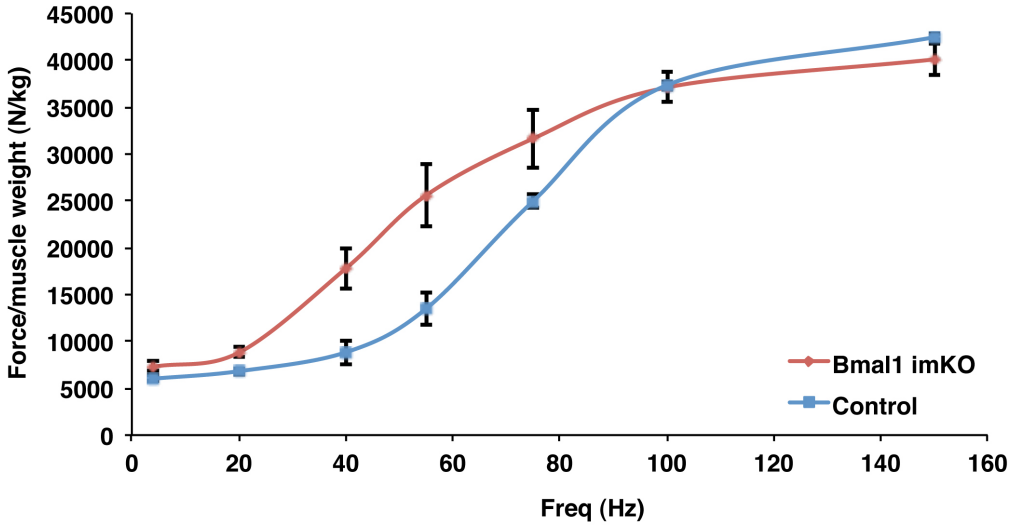

Figure 22. Force measurements: Stimulation of the Gastrocnemius muscle in *Bmal1* imKO and controls. **A**. Absolute force (force: g, frequency of the stimulus: Hz). **B**. Normalized force by body weight (N/Kg, Hz) (Student's t−test).

6 DISCUSSION

6.1 *Bmal1* deletion in whole body and in skeletal muscle

BMAL1 is known to be an essential component of both central and peripheral clocks. Deletion of *Bmal1* specifically in skeletal muscle (*Bmal1* mKO) allows us to investigate its role in muscle physiology without confounding whole−body effects. Unlike *Bmal1*$^{-/-}$ mice, *Bmal1* mKO mice show normal locomotor activity at night, demonstrating that the light input from the retina to the SCN and the circadian entrainment is conserved.

Ablation of the clock gene *Bmal1* at the whole body level causes reduced lifespan, body weight, muscle mass and loss of circadian locomotor activity (Kondratov *et al*., 2006; Bunger *et al.*, 2000). Rescue experiments in *Bmal1* null mice showed that re−expression of *Bmal1* in the brain restores the periodicity of the activity but not its total levels, while rescue in skeletal muscle, albeit at constitutively high levels, restored total activity levels without restoring rhythmicity (McDearmon *et al.,* 2006). Our findings show that local ablation of *Bmal1* in skeletal muscle does not decrease lifespan or body weight, and in contrast with the findings in *Bmal1* null mice, circadian activity rhythms in *Bmal1* mKO and *Bmal1* imKO mice were preserved (**Figure 10** and **Figure 21**). Surprisingly, the level of activity in *Bmal1* mKO mice during the night was increased by approximately 20% compared to controls, whereas this difference was not seen in *Bmal1* imKO mice (**Figure 21**).

6.2 The effect of *Bmal1* mKO on the muscle core clock

The response of the core clock genes (**Figure 14** and **Figure 15**) to the local ablation of *Bmal1* is consistent with previous results in *Bmal1* null mice and *Bmal1* liver−specific knockout (Kondratov *et al.*, 2006; Lamia *et al.*, 2008). The fact that *Per2* oscillation is almost unchanged in *Bmal1* mKO muscles may reflect a role for oscillating systemic signals in the regulation of this gene, as demonstrated in liver−specific *Bmal1* knockout (Buhr *et al., 2010;* Kornmann et al., 2007). The up−regulation of *Clock*, *Cry* and *E4bp4* in *Bmal1* mKO muscles

may be due to the lack of repression (Kondratov *et al.,* 2006). The fact that targets of E4BP4 and HLF were down−regulated (**Figure 6**) is in agreement with the changes in their transcript levels. HLF is a transcriptional activator, as well as a direct target gene of CLOCK:BMAL1, and its transcript levels are markedly reduced in *Bmal1* mKO muscles. On the other hand, E4BP4 is a transcriptional repressor, and its transcript levels are markedly increased in the absence of muscle BMAL1, presumably leading to increased repression of its targets. In addition, the conserved rhythmic oscillation of other genes, such as *Per2*, reflects a possible regulation by extrinsic factors in the absence of *Bmal1*. Previous studies have shown that through heat shock response pathways, temperature acts as an entrainment signal for circadian rhythms in peripheral clocks, consistent with the binding of Heat Shock Factor 1 (HSF1) to heat shock−binding elements within the upstream region of the *Per2* gene (Buhr *et al.*, 2010), thus driving the oscillatory pattern of *Per2* transcript even in the absence of CLOCK:BMAL1−dependent transcription.

6.3 BMAL1 and MyoD

MyoD, a myogenic regulatory factor, has been identified as a circadian gene with a peak of expression in the subjective night (McCarthy *et al.,* 2007). Circadian expression of *Myod1,* the gene coding for MyoD*,* was lost in *Bmal1* null mice and it was suggested that *Myod1* is a direct target of the core clock based on the finding that BMAL1 binds the *Myod1* promoter and that *Bmal1* KO and MyoD KO mice show similar changes in muscle structure and function (Andrews *et al.,* 2010). However, our results show that *Bmal1* mKO muscle maintain a circadian pattern of expression for *Myod1* and even increased levels of *Myod1* expression at some time points (**Figure 16**B). These findings suggest that *Myod1* oscillation is mainly controlled by systemic circadian cues.

6.4 *Bmal1*, muscle structure and muscle function

Intriguingly, whole body *Bmal1* null mice show a very strong muscle phenotype, with marked decrease in muscle mass and muscle force due to severe alterations in muscle morphology (Kondratov *et al.,* 2006, Andrews *et al.,* 2010). In contrast,

in our muscle−specific *Bmal1* mKO model, muscle structure was normal and muscle mass was actually increased (**Figure 6**). In addition, similar to *Bmal1* null mice, both absolute force and normalized force were depressed compared to control muscles (**Figure 11**). The hypothesis that muscle force decrease is due to an altered myofibrillar architecture based on analyses in *Bmal1* null mice (Andrews *et al.,* 2010) was not corroborated in our studies of the *Bmal1* mKO (**Figure 8**).

On the other hand, we found that some of the changes in muscle composition and muscle function of the *Bmal1* mKO are comparable to the changes observed in *myostatin* null mice ($mstn^{-/-}$). In particular, both knockout models show a change in fiber−type profile, with a tendency toward fast type muscle fibers (Girgenrath *et al.,* 2005), and an increased muscle mass yet impaired force production (Amthor *et al.*, 2007; McPherron *et al.*, 2009). Myostatin is a member of the Transforming Growth Factor−β (TGFβ) superfamily, and a negative regulator of muscle growth, therefore the lack of myostatin leads to an increase in muscle growth. Myostatin binds a receptor complex composed of activin receptor 2B and activin receptor 1B, also called Alk4, whose activation leads to the phosphorylation and nuclear translocation of Smad2 and Smad3 transcription factors (Sartori *et al.,* 2009). Interestingly, *Acvr1b*, which encodes for Alk4, was shown to be a clock−dependent circadian gene whose circadian expression and transcript levels are abrogated in *Bmal1* mKO muscles (**Figure 16**).

Our findings would suggest a possible regulatory role for the intrinsic muscle clock in the myostatin–activin receptor–Smad pathway, and thus on muscle protein synthesis and muscle growth. Indeed, it has recently been shown that the circadian clock orchestrates the organization of transcriptional and translational processes in liver, modulating transcription of rRNAs, ribosomal protein synthesis and ribosome biogenesis, and related signaling pathways, therefore controls protein synthesis (Jouffe *et al.*, 2013).

6.6 p38 pathway

Different lines of evidence from our microarray analysis indicate that the mitogen activated protein kinase (MAPK) p38 pathway is down−regulated in *Bmal1* mKO muscles. The MAPK p38 pathway is involved in the response to different stress signaling stimuli, physical exercise and skeletal muscle contraction (Boppart *et al*., 2001; Akimoto *et al*., 2005). In cardiac muscle, it was described that phosphorylated p38 MAPK, the activated protein, shows a robust rhythmicity, which was lost in animals with a disrupted circadian core clock, suggesting that cardiac p38 may be under the influence of local cardiac clock (Ko *et al.,* 2011).

At the molecular level, p38 is activated via phosphorylation by the mitogen activated kinase kinase MKK6, the converging point of activation by external stimuli (**Figure 23**). In turn, activated p38 phosphorylates a wide range of substrates, such as the Activating Transcription Factor 2 (ATF2), Myocite Enhancer Factor 2C (MEF2C), and, through other kinases, cAMP responsive element−binding protein (CREB), Nuclear factor−KappaB (NF−κB) and others. We have observed that in *Bmal1* mKO mice the p38 pathway is altered at different points (**Table 7**): *Map2k6* transcripts, which code for MKK6, the upstream activator of p38, were down−regulated (**Figure 17**), and according to GSEA, many transcriptional targets of p38−dependent transcription factors, like ATF2 or MEF2C, were also down−regulated (**Table 6**). Thus all these data point to a reduced activity of the p38 pathway in the absence of *Bmal1* in skeletal muscle. Since the p38 pathway was shown to be stimulated by contractile activity (Boppart *et al*., 2001; Akimoto *et al*., 2005), we hypothesize that the clock machinery may prepare the muscles for the awake/activity phase. If this interpretation is correct and confirmed by studies at the protein level, we would predict that the *Bmal1* mKO mice should have reduced physical adaptation abilities in response to exercise.

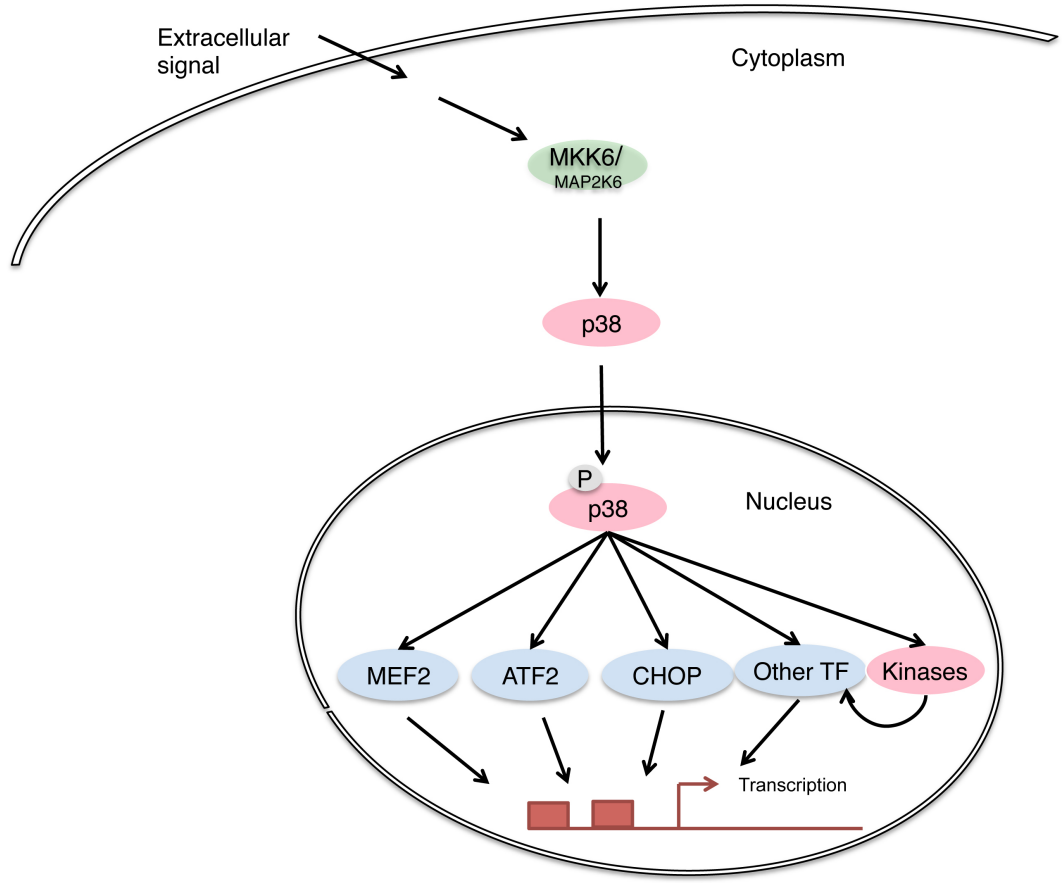

Figure 23. Schematic representation of the p38 MAPK pathway.

6.7 Future perspectives

In order to validate whether the various signaling pathways suggested by our preliminary microarray analysis are in fact affected by the ablation of *Bmal1*, it will be important to study the muscle circadian proteome, and to correlate the changes observed at the transcript level with those at the protein level. However, a complete analysis must also take into account various posttranslational modifications, such as phosphorylation or ubiquitination, which would affect localization, activity and half−life of these proteins.

Elucidation of the role played by *Bmal1* in the regulation of the p38 pathway should be first validated by western blot analyses of the key members of the pathway at precise time points, looking at the total protein levels as well as the active/phosphorylated protein levels. In order to understand whether the adaptive ability of the muscles is compromised by the skeletal muscle ablation of *Bmal1*, we suggest subjecting the animals to contractile stimulation, either

by voluntary−running or direct electrical stimulation of the sciatic nerve, and to analyze the response of the muscles to this mechanical stress. In parallel, it will be of interest to study the response of the muscle structural machinery to the mechanical stimulation, and particularly to eccentric contractions, which are known to reveal hidden vulnerability of altered muscles.

Most experiments we conducted were done in the *Bmal1* mKO model; in consequence it is possible that some of the differences we have observed are caused by compensatory mechanisms due to the lack of BMAL1 during postnatal development. Therefore, it would be of great interest to first confirm the changes in the circadian gene expression profile in the inducible muscle−specific *Bmal1* KO model (imKO) by microarray analyses and/or RT−qPCR.

REFERENCES

Akashi M, Takumi T. The orphan nuclear receptor RORalpha regulates circadian transcription of the mammalian core-clock Bmal1. *Nature structural & molecular biology* 12: 441–8, 2005.

Akimoto T, Pohnert SC, Li P, Zhang M, Gumbs C, Rosenberg PB, Williams RS, Yan Z. Exercise stimulates Pgc-1alpha transcription in skeletal muscle through activation of the p38 MAPK pathway. *The Journal of biological chemistry* 280: 19587–93, 2005.

Albrecht U, Sun ZS, Eichele G, Lee CC. A differential response of two putative mammalian circadian regulators, mper1 and mPer2, to light. *Cell* 91: 1055–64, 1997.

Albrecht U. Orchestration of gene expression and physiology by the circadian clock. *Journal of physiology, Paris* 100: 243–51, 2007.

Amthor H, Macharia R, Navarrete R, Schuelke M, Brown SC, Otto A, Voit T, Muntoni F, Vrbóva G, Partridge T, Zammit P, Bunger L, Patel K. Lack of myostatin results in excessive muscle growth but impaired force generation. *Proceedings of the National Academy of Sciences of the United States of America* 104: 1835–40, 2007.

Andrews JL, Zhang X, McCarthy JJ, McDearmon EL, Hornberger T A, Russell B, Campbell KS, Arbogast S, Reid MB, Walker JR, Hogenesch JB, Takahashi JS, Esser K A. CLOCK and BMAL1 regulate MyoD and are necessary for maintenance of skeletal muscle phenotype and function. *Proceedings of the National Academy of Sciences of the United States of America* 107: 19090–5, 2010.

Asher G, Schibler U. Crosstalk between components of circadian and metabolic cycles in mammals. *Cell metabolism* 13: 125–37, 2011.

Baker J, Riley G, Romero MR, Haynes AR, Hilton H, Simon M, Hancock J, Tateossian H, Ripoll VM, Blanco G. Identification of a Z-band associated protein complex involving KY, FLNC and IGFN1. *Experimental cell research* 316: 1856–70, 2010.

Balsalobre A, Brown SA, Marcacci L, Tronche F, Kellendonk C, Reichardt HM, Schütz G, Schibler U. Resetting of circadian time in peripheral tissues by glucocorticoid signaling. *Science* 289: 2344–7, 2000.

Berson DM, Dunn F A, Takao M. Phototransduction by retinal ganglion cells that set the circadian clock. *Science* 295: 1070–3, 2002.

Blaauw B, Canato M, Agatea L, Toniolo L, Mammucari C, Masiero E, Abraham R, Sandri M, Schiaffino S, Reggiani C. Inducible activation of Akt increases skeletal muscle mass and force without satellite cell activation. *FASEB journal : official publication of the Federation of American Societies for Experimental Biology* 23: 3896–905, 2009.

REFERENCES

Blaauw B, Mammucari C, Toniolo L, Agatea L, Abraham R, Sandri M, Reggiani C, Schiaffino S. Akt activation prevents the force drop induced by eccentric contractions in dystrophin-deficient skeletal muscle. *Human molecular genetics* 17: 3686–96, 2008.

Boden MJ, Varcoe TJ, Voultsios A, Kennaway DJ. Reproductive biology of female Bmal1 null mice. *Reproduction* 139: 1077–90, 2010.

Boppart MD, Hirshman MF, Sakamoto K, Fielding RA, Goodyear LJ. Static stretch increases c-Jun NH2-terminal kinase activity and p38 phosphorylation in rat skeletal muscle. *American journal of physiology. Cell physiology* 280: C352–8, 2001.

Bothe GW, Haspel J a, Smith CL, Wiener HH, Burden SJ. Selective expression of Cre recombinase in skeletal muscle fibers. *Genesis* 26: 165−6, 2000.

Buhr ED, Yoo S-H, Takahashi JS. Temperature as a universal resetting cue for mammalian circadian oscillators. *Science* 330: 379–85, 2010.

Bunger MK, Wilsbacher LD, Moran SM, Clendenin C, Radcliffe L a, Hogenesch JB, Simon MC, Takahashi JS, Bradfield C a. Mop3 is an essential component of the master circadian pacemaker in mammals. *Cell* 103: 1009–17, 2000.

Busino L, Bassermann F, Maiolica A, Lee C, Nolan PM, Godinho SIH, Draetta GF, Pagano M. SCFFbxl3 controls the oscillation of the circadian clock by directing the degradation of cryptochrome proteins. *Science* 316: 900–4, 2007.

Cardone L, Hirayama J, Giordano F, Tamaru T, Palvimo JJ, Sassone-Corsi P. Circadian clock control by SUMOylation of BMAL1. *Science* 309: 1390–4, 2005.

Conesa A, Nueda MJ, Ferrer A, Talón M. maSigPro: a method to identify significantly differential expression profiles in time-course microarray experiments. *Bioinformatics* 22: 1096–102, 2006.

Dai M, Wang P, Boyd AD, Kostov G, Athey B, Jones EG, Bunney WE, Myers RM, Speed TP, Akil H, Watson SJ, Meng F. Evolving gene/transcript definitions significantly alter the interpretation of GeneChip data. *Nucleic acids research* 33: e175, 2005.

Damiola F, Le Minh N, Preitner N, Kornmann B, Fleury-Olela F, Schibler U. Restricted feeding uncouples circadian oscillators in peripheral tissues from the central pacemaker in the suprachiasmatic nucleus. *Genes & development* 14: 2950–61, 2000.

Dibner C, Schibler U, Albrecht U. The mammalian circadian timing system: organization and coordination of central and peripheral clocks. *Annual review of physiology* 72: 517–49, 2010.

Eide EJ, Vielhaber EL, Hinz W a, Virshup DM. The circadian regulatory proteins BMAL1 and cryptochromes are substrates of casein kinase Iepsilon. *The Journal of biological chemistry* 277: 17248–54, 2002.

Gallego M, Virshup DM. Post-translational modifications regulate the ticking of the circadian clock. *Nature reviews. Molecular cell biology* 8: 139–48, 2007.

Gekakis N, Staknis D, Nguyen HB, Davis FC, Wilsbacher LD, King DP, Takahashi JS, Weitz CJ. Role of the CLOCK Protein in the Mammalian Circadian Mechanism. *Science* 280: 1564–1569, 1998.

Girgenrath S, Song K, Whittemore L-A. Loss of myostatin expression alters fiber-type distribution and expression of myosin heavy chain isoforms in slow- and fast-type skeletal muscle. *Muscle & nerve* 31: 34–40, 2005.

Godinho SIH, Maywood ES, Shaw L, Tucci V, Barnard AR, Busino L, Pagano M, Kendall R, Quwailid MM, Romero MR, O'neill J, Chesham JE, Brooker D, Lalanne Z, Hastings MH, Nolan PM. The after-hours mutant reveals a role for Fbxl3 in determining mammalian circadian period. *Science* 316: 897–900, 2007.

Griffin EA, Staknis D, Weitz CJ. Light-independent role of CRY1 and CRY2 in the mammalian circadian clock. *Science* 286: 768–71, 1999.

Hirota T, Okano T, Kokame K, Shirotani-Ikejima H, Miyata T, Fukada Y. Glucose down-regulates Per1 and Per2 mRNA levels and induces circadian gene expression in cultured Rat-1 fibroblasts. *The Journal of biological chemistry* 277: 44244–51, 2002.

Hogenesch JB, Gu YZ, Jain S, Bradfield CA. The basic-helix-loop-helix-PAS orphan MOP3 forms transcriptionally active complexes with circadian and hypoxia factors. *Proceedings of the National Academy of Sciences of the United States of America* 95: 5474–9, 1998.

Hughes ME, Hogenesch JB, Kornacker K. JTK_CYCLE: an efficient nonparametric algorithm for detecting rhythmic components in genome-scale data sets. *Journal of biological rhythms* 25: 372–80, 2010.

Jones CR, Campbell SS, Zone SE, Cooper F, DeSano A, Murphy PJ, Jones B, Czajkowski L, Ptácek LJ. Familial advanced sleep-phase syndrome: A short-period circadian rhythm variant in humans. *Nature medicine* 5: 1062–5, 1999.

Jouffe C, Cretenet G, Symul L, Martin E, Atger F, Naef F, Gachon F. The circadian clock coordinates ribosome biogenesis. *PLoS biology* 11: e1001455, 2013.

Ko ML, Shi L, Tsai J-Y, Young ME, Neuendorff N, Earnest DJ, Ko GY-P. Cardiac-specific mutation of Clock alters the quantitative measurements of physical activities without changing behavioral circadian rhythms. *Journal of biological rhythms* 26: 412–22, 2011.

Kondratov R V, Kondratova AA, Gorbacheva VY, Vykhovanets O V, Antoch MP. Early aging and age-related pathologies in mice deficient in BMAL1, the core componentof the circadian clock. *Genes & development* 20: 1868–73, 2006.

Kondratov R V, Shamanna RK, Kondratova A a, Gorbacheva VY, Antoch MP. Dual role of the CLOCK/BMAL1 circadian complex in transcriptional regulation. *FASEB journal : official publication of the Federation of American Societies for Experimental Biology* 20: 530–2, 2006.

Kornmann B, Schaad O, Bujard H, Takahashi JS, Schibler U. System-driven and oscillator-dependent circadian transcription in mice with a conditionally active liver clock. *PLoS biology* 5: e34, 2007.

Lamia K a, Storch K-F, Weitz CJ. Physiological significance of a peripheral tissue circadian clock. *Proceedings of the National Academy of Sciences of the United States of America* 105: 15172–7, 2008.

4**Lehman MN, Silver R, Gladstone WR, Kahn RM, Gibson M, Bittman EL**. Circadian rhythmicity restored by neural transplant. Immunocytochemical characterization of the graft and its integration with the host brain. *The Journal of neuroscience : the official journal of the Society for Neuroscience* 7: 1626–38, 1987.

Liu AC, Tran HG, Zhang EE, Priest A a, Welsh DK, Kay S a. Redundant function of REV-ERBalpha and beta and non-essential role for Bmal1 cycling in transcriptional regulation of intracellular circadian rhythms. *PLoS genetics* 4: e1000023, 2008.

Lowrey PL, Shimomura K, Antoch MP, Yamazaki S, Zemenides PD, Ralph MR, Menaker M, Takahashi JS. Positional syntenic cloning and functional characterization of the mammalian circadian mutation tau. *Science* 288: 483–92, 2000.

McCarthy JJ, Andrews JL, McDearmon EL, Campbell KS, Barber BK, Miller BH, Walker JR, Hogenesch JB, Takahashi JS, Esser KA. Identification of the circadian transcriptome in adult mouse skeletal muscle. *Physiological genomics* 31: 86–95, 2007.

McDearmon EL, Patel KN, Ko CH, Walisser J a, Schook AC, Chong JL, Wilsbacher LD, Song EJ, Hong H-K, Bradfield C a, Takahashi JS. Dissecting the functions of the mammalian clock protein BMAL1 by tissue-specific rescue in mice. *Science (New York, N.Y.)* 314: 1304–8, 2006.

McPherron AC, Huynh T V, Lee S-J. Redundancy of myostatin and growth/differentiation factor 11 function. *BMC developmental biology* 9: 24, 2009.

Mitsui S, Yamaguchi S, Matsuo T, Ishida Y, Okamura H. Antagonistic role of E4BP4 and PAR proteins in the circadian oscillatory mechanism. *Genes & development* 15: 995–1006, 2001.

Preitner N, Damiola F, Lopez-Molina L, Zakany J, Duboule D, Albrecht U, Schibler U. The orphan nuclear receptor REV-ERBalpha controls circadian transcription within the positive limb of the mammalian circadian oscillator. *Cell* 110: 251–60, 2002.

Sanada K, Okano T, Fukada Y. Mitogen-activated protein kinase phosphorylates and negatively regulates basic helix-loop-helix-PAS transcription factor BMAL1. *The Journal of biological chemistry* 277: 267–71, 2002.

Sandonà D, Desaphy J-F, Camerino GM, Bianchini E, Ciciliot S, Danieli-Betto D, Dobrowolny G, Furlan S, Germinario E, Goto K, Gutsmann M, Kawano F, Nakai N, Ohira T, Ohno Y, Picard A, Salanova M, Schiffl G, Blottner D, Musarò A, Ohira Y, Betto R, Conte D, Schiaffino S. Adaptation of mouse skeletal muscle to long-term microgravity in the MDS mission. *PloS one* 7: e33232, 2012.

Sartori R, Milan G, Patron M, Mammucari C, Blaauw B, Abraham R, Sandri M. Smad2 and 3 transcription factors control muscle mass in adulthood. *American journal of physiology. Cell physiology* 296: C1248–57, 2009.

Sato TK, Panda S, Miraglia LJ, Reyes TM, Rudic RD, McNamara P, Naik K a, FitzGerald G a, Kay S a, Hogenesch JB. A functional genomics strategy reveals Rora as a component of the mammalian circadian clock. *Neuron* 43: 527–37, 2004.

Schiaffino S, Gorza L, Sartore S, Saggin L, Ausoni S, Vianello M, Gundersen K, Lømo T. Three myosin heavy chain isoforms in type 2 skeletal muscle fibres. *Journal of muscle research and cell motility* 10: 197–205, 1989.

Schiaffino S. Fibre types in skeletal muscle: a personal account. *Acta physiologica* 199: 451–63, 2010.

Schuler M, Ali F, Metzger E, Chambon P, Metzger D. Temporally controlled targeted somatic mutagenesis in skeletal muscles of the mouse. *Genesis* 41: 165–70, 2005.

Shearman LP, Sriram S, Weaver DR, Maywood ES, Chaves I, Zheng B, Kume K, Lee CC, Van der Horst GT, Hastings MH, Reppert SM. Interacting molecular loops in the mammalian circadian clock. *Science* 288: 1013–9, 2000.

Siepka SM, Yoo S-H, Park J, Song W, Kumar V, Hu Y, Lee C, Takahashi JS. Circadian mutant Overtime reveals F-box protein FBXL3 regulation of cryptochrome and period gene expression. *Cell* 129: 1011–23, 2007.

Stephan FK, Zucker I. Circadian rhythms in drinking behavior and locomotor activity of rats are eliminated by hypothalamic lesions. *Proceedings of the National Academy of Sciences of the United States of America* 69: 1583–6, 1972.

Stokkan K a, Yamazaki S, Tei H, Sakaki Y, Menaker M. Entrainment of the circadian clock in the liver by feeding. *Science* 291: 490–3, 2001.

Storch K-F, Paz C, Signorovitch J, Raviola E, Pawlyk B, Li T, Weitz CJ. Intrinsic circadian clock of the mammalian retina: importance for retinal processing of visual information. *Cell* 130: 730–41, 2007.

Subramanian A, Tamayo P, Mootha VK, Mukherjee S, Ebert BL, Gillette MA, Paulovich A, Pomeroy SL, Golub TR, Lander ES, Mesirov JP. Gene set enrichment analysis: a knowledge-based approach for interpreting genome-wide expression profiles. *Proceedings of the National Academy of Sciences of the United States of America* 102: 15545–50, 2005.

Sun ZS, Albrecht U, Zhuchenko O, Bailey J, Eichele G, Lee CC. RIGUI, a putative mammalian ortholog of the Drosophila period gene. *Cell* 90: 1003–11, 1997.

Takano a, Shimizu K, Kani S, Buijs RM, Okada M, Nagai K. Cloning and characterization of rat casein kinase 1epsilon. *FEBS letters* 477: 106−12, 2000.

Travnickova-Bendova Z, Cermakian N, Reppert SM, Sassone-Corsi P. Bimodal regulation of mPeriod promoters by CREB-dependent signaling and CLOCK/BMAL1 activity. *Proceedings of the National Academy of Sciences of the United States of America* 99: 7728–33, 2002.

Vanselow K, Vanselow JT, Westermark PO, Reischl S, Maier B, Korte T, Herrmann A, Herzel H, Schlosser A, Kramer A. Differential effects of PER2 phosphorylation: molecular basis for the human familial advanced sleep phase syndrome (FASPS). *Genes & development* 20: 2660–72, 2006.

Yamaguchi S, Mitsui S, Yan L, Yagita K, Miyake S, Okamura H. Role of DBP in the circadian oscillatory mechanism. *Molecular and cellular biology* 20: 4773–81, 2000.

Yoo S-H, Yamazaki S, Lowrey PL, Shimomura K, Ko CH, Buhr ED, Siepka SM, Hong H-K, Oh WJ, Yoo OJ, Menaker M, Takahashi JS. PERIOD2::LUCIFERASE real-time reporting of circadian dynamics reveals persistent circadian oscillations in mouse peripheral tissues. *Proceedings of the National Academy of Sciences of the United States of America* 101: 5339–46, 2004.

UNIVERSITÀ DEGLI STUDI DI PADOVA

SCUOLA DI DOTTORATO
IN BIOSCIENZE E BIOTECNOLOGIE
INDIRIZZO DI GENETICA E BIOLOGIA
MOLECOLARE DELLO SVILUPPO

Verbale del Collegio dei Docenti dell'Indirizzo in "Genetica e Biologia Molecolare dello Sviluppo", Scuola di Dottorato in Bioscienze e Biotecnologie, Università di Padova

Il giorno lunedì 3 dicembre 2012 alle ore 12.00 si è riunito per via telematica il Collegio dei Docenti dell'Indirizzo di "Genetica e Biologia Molecolare dello Sviluppo" della Scuola di Dottorato in Bioscienze e Biotecnologie.

Ordine del giorno:

1. Approvazione del passaggio all'anno successivo dei dottorandi iscritti al XXVI e XXVII ciclo.
2. Giudizio sull'attività triennale dei dottorandi iscritti al XXV ciclo ed ammissione all'esame finale per il conseguimento del titolo.

1. Sulla base delle relazioni annuali dei dottorandi, svoltesi nei giorni 26.11.2012, 27.11.2012, 28.11.2012, 29.11.2012 e 30.11.2012, il Collegio dei Docenti approva all'unanimità il passaggio all'anno successivo dei dottorandi iscritti ai suddetti cicli:

   XXVI ciclo: Casari Alessandro, Corallo Diana, Gregianin Elisa, Nuzzo Simona, Piazzesi Antonia, Verma Narendra.

   XXVII ciclo: Andreatta Gabriele, Astone Matteo, Castagnaro Silvia, Chen Peiwen, Cieri Domenico, Coassin Silvia, Ek Olivier, Renesto Alice, Zancan Ilaria.

2. Sulla base del lavoro svolto durante il ciclo triennale di studi e ricerche, e della dettagliata relazione presentata da ciascuno dei dottorandi del XXV ciclo in data 26.11.2012, 27.11.2012, 28.11.2012 e 30.11.2012, il Collegio dei Docenti ritiene che tutti gli allievi abbiano conseguito risultati di rilevante valore scientifico ed esprime un giudizio positivo sull'attività svolta da ciascuno di essi. Sulla base di tali giudizi, il Collegio Docenti propone che gli **allievi Busolin Giorgia, Calura Enrica, Galletta Eva, Gumeni Sentiljana, Peña Paz Ivonne, Schiesari Luca, Tosoni Elena, Vallese Dennis** vengano ammessi a sostenere l'esame finale per il conseguimento del titolo.

Non essendoci altri argomenti da discutere, la seduta è tolta alle ore 13.00.

Il Coordinatore

Prof. Paolo Bonaldo

Direttore Prof. Giuseppe Zanotti
Sede amministrativa:
Dipartimento di Biologia c/o complesso Biologico Interdipartimentale "A. Vallisneri"
Via U. Bassi 58/b – 35131 Padova (Italy)

DIPARTIMENTO DI BIOLOGIA
Viale G. Colombo 3 / Via U. Bassi 58/b
35131 Padova
Tel +39 049 8276178
Fax +39 049 8072213
E-mail: *direbiol@bio.unipd.it*
CF: 80006480281; P. IVA: 00742430283

UNIVERSITÀ DEGLI STUDI DI PADOVA

PhD student: Marcia Ivonne Pena Pax

Tutor: Prof. Gerolamo Lanfranchi

Marcia Ivonne Pena Paz ha svolto il triennio di dottorato di ricerca quale borsista Marie Curie nell'ambito del consorzio internazionale "MUZIC" finanziato dall'Unione Europea nel progetto PEOPLE del 7° programma quadro. Del consorzio fanno parte il sottoscritto ed il Prof. Stefano Schiaffino dell'Istituto Veneto di medicina Molecolare di Padova, e a ciascuno di noi il consorzio ha asegnato una borsa arie Curie per dottorandi. Marcia Ivonne Pena Paz ha svolto quindi il progetto di ricerca del suo dottorato sotto la guida del prof. Stefano Schiaffino.

Ho potuto seguire regolarmente il lavoro scientifico di Ivonne con incontri di discussione e programmazione, visti anche gli assidui rapporti collaborativi con il Prof. Schiaffino.

Il mio giudizio sul lavoro svolto e sulla personalità di Marcia Ivonne Pena Paz è molto positivo e posso affermare di concordare appieno con la relazione estesa presentata in allegato dal Prof. Schiaffino, responsabile del progetto di ricerca di dottorato di Ivonne.

Gerolamo Lanfranchi
Professore di Genetica
Dipartimento di Biologia
Università di Padova

Fondazione per la Ricerca Biomedica Avanzata
Foundation for Advanced Biomedical Research
(VIMM)

Istituto Veneto di Medicina Molecolare
Venetian Institute of Molecular Medicine

Padova, 18 gennaio 2013

Rapporto sulla dottoranda Marcia Ivonne Peña Paz

Marcia Ivonne Peña Paz ha svolto il dottorato di ricerca nel mio laboratorio dopo aver ottenuto una borsa Marie Curie nell'ambito del network europeo FP7 Initial Training Network (ITN) MUZIC, a cui sono associato insieme al Prof. G. Lanfranchi. Nel corso di dottorato Ivonne ha lavorato su un progetto di ricerca relativo alla inattivazione del gene circadiano *Bmal1* nel muscolo scheletrico. Questo progetto ha previsto la generazione di due ceppi di topi knockout utilizzando il sistema Cre-LoxP. Nel primo modello, topi *Bmal1-floxed* sono stati incrociati con topi *Mlc1f-Cre*, in cui la Cre ricombinasi è controllata del gene muscolo-specifico *myosin light chain 1f*, per cui l'incrocio causa l'inattivazione di *Bmal1* nel muscolo sin da stadi precoci dello sviluppo. Nel secondo modello, i topi *Bmal1-floxed* sono stati incrociati con topi *HSA-Cre-ER*, in cui la *Cre ricombinasi*, legata a un recettore per gli estrogeni mutato, è controllata dal gene muscolo-specifico *human skeletal actin*, per cui l'incrocio causa l'inattivazione di *Bmal1* nel muscolo scheletrico solo nell'animale adulto dopo trattamento con tamoxifen. Un importante risultato di questo studio è che la rottura del ritmo circadiano intrinseco del muscolo, conseguente all'inattivazione di *Bmal1*, causa resistenza all'insulina e disregolazione metabolica con alterazione del metabolismo di carboidrati, lipidi ed amino acidi nel muscolo scheletrico. Il lavoro che descrive questi effetti, di cui Ivonne è coautore, è stato inviato per pubblicazione a *Cell Metabolism*. Altri risultati di questo progetto saranno oggetto di ulteriori pubblicazioni.

Sotto la diretta supervisione dei miei collaboratori Bert Blaauw e Ken Dyar, Ivonne ha contribuito in modo importante alle diverse fasi di questo progetto complesso, dagli incroci dei topi con determinazione del genotipo all'analisi di espressione genica mediante microarray, PCR quantitativa e immunoblotting, fino alle analisi della distribuzione di proteine specifiche mediante immunofluorescenza. Nelle prime fasi del suo apprendistato in laboratorio ha inoltre acquisito esperienza nell'isolamento e nello studio di singole fibre da muscoli di topo adulto.

Ivonne ha presentato periodicamente i risultati del suo lavoro alle riunioni annuali del consorzio ITN-MUZIC, oltre che agli incontri della scuola di dottorato di Padova, e ha frequentato i numerosi Workshops e Summer Schools organizzati da ITN-MUZIC (v. allegato). Nel congresso EMC 2012 (41st European Muscle Conference), tenutosi a Rodi nel settembre 2012, Ivonne ha presentato un abstract sul suo lavoro che è stato molto apprezzato, tanto da essere selezionato per la presentazione orale e da meritare il premio della European Society for Muscle Research ("ESMR Young Investigator Award") destinato a studenti di dottorato e giovani postdoc.

Nel complesso giudico molto positivamente il lavoro svolto da Ivonne come studente di dottorato e mi auguro che l'esperienza acquisita le sia utile per la sua attività futura.

Stefano Schiaffino
Professore Emerito dell'Università di Padova
Group Leader presso l'Istituto Veneto di Medicina Molecolare

Stefano Schiaffino
Venetian Institute of Molecular Medicine (VIMM)
Via Orus 2
35129 Padova
Italy
E-mail: stefano.schiaffino@unipd.it
Tel: 049-7923232
Fax: 049-7923250

Fondazione per la Ricerca Biomedica Avanzata
Foundation for Advanced Biomedical Research (VIMM)

Istituto Veneto di Medicina Molecolare
Venetian Institute of Molecular Medicine

Allegato rapporto dottoranda Marcia Ivonne Peña Paz: partecipazione a workshops/summer schools MUZIC e altri meetings (2010-12)

MUZIC workshops/summer schools		
Gene Silencing	Padua, Italy	October 2012
Scientific English	Padua, Italy	October 2012
Protein – Protein interaction	London, England	June 2012
Electron Microscopy and Tomography	Leeds, England	March 2012
Advance fluorescence microscopy	Bonn, Germany	November 2012
Summer School-Basic Fluorescence Microscopy	Jyvaskyla, Finland	August 2011
X-ray structure determination	Hamburg, Germany	June 2011
Proteopedia	Hamburg, Germany	June 2011
Communication with public, EMBL	Hamburg, Germany	June 2011
Biphysical characterization and crystallisation	Vienna, Austria	November 2010
Oral communication skills	Vienna, Austria	November 2010
Other meetings/congresses		
41st European Muscle Conference (speaker, Young Investigator Award)	Rhodes, Greece	September 2012
MyoAge (speaker)	Barcelona, Spain	December 2011
MyoAge	Padua, Italy	October 2010
39th European Muscle Conference	Padua, Italy	September 2010